OFFICE OF SCIENTIFIC RESEARCH & DEVELOPMENT
NATIONAL DEFENSE RESEARCH COMMITTEE
DIVISION SIX - SECTION 6.1

NOSE CAVITATION OGIVES AND SPHEROGIVES

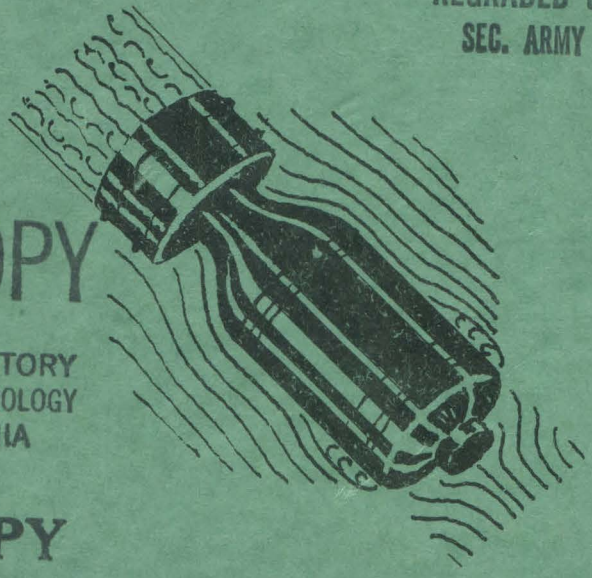

THE HIGH SPEED WATER TUNNEL
CALIFORNIA INSTITUTE OF TECHNOLOGY
PASADENA, CALIFORNIA

SECTION Nº 6.1-sr 207-1906
HML Nº ND 31.1

COPY Nº 95

OFFICE OF SCIENTIFIC RESEARCH AND DEVELOPMENT
NATIONAL DEFENSE RESEARCH COMMITTEE
DIVISION SIX — SECTION 6.1

NOSE CAVITATION

OGIVES AND SPHEROGIVES

BY
ROBERT T. KNAPP
OFFICIAL INVESTIGATOR

THE HIGH SPEED WATER TUNNEL
AT THE
CALIFORNIA INSTITUTE OF TECHNOLOGY
HYDRAULIC MACHINERY LABORATORY
PASADENA, CALIFORNIA

Section No. 6.1-sr207-1906
HML No. ND-31.1

Report Prepared by
Harold L. Doolittle
Hydraulic Engineer

January 18, 1945

TABLE OF CONTENTS

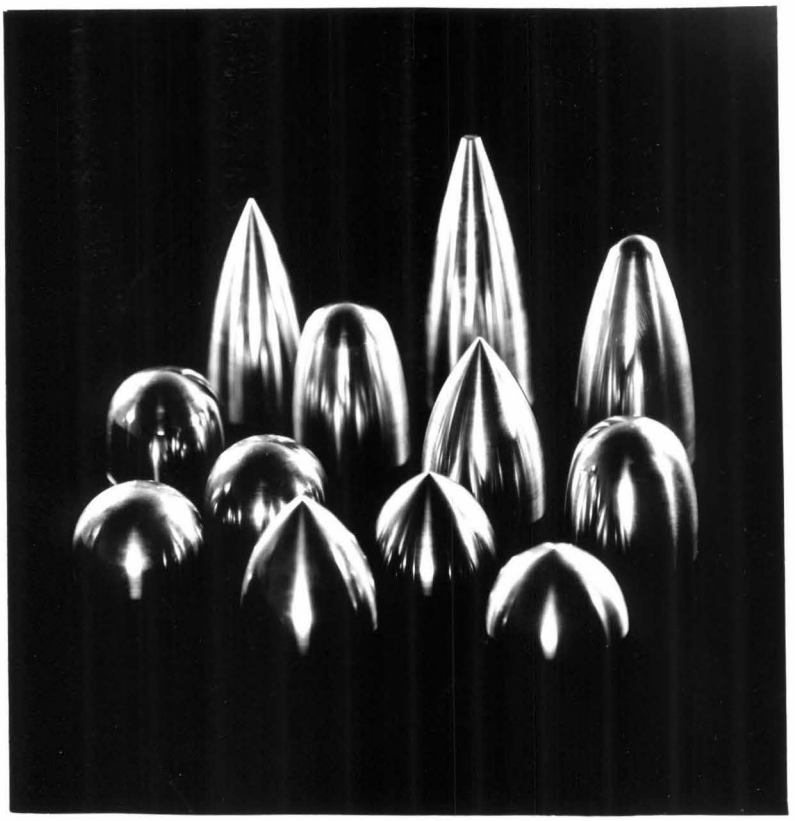

OGIVES
AND
SPHEROGIVES

NOSE CAVITATION

OGIVES AND SPHEROGIVES

GENERAL

This report covers the progress made to date on an investigation of cavitation on various projectile nose shapes. It is closely allied with and supplements the report by Dr. R. T. Knapp, entitled "Entrance and Cavitation Bubbles", No. 6.1-sr207-1900, dated December 27, 1944. All work reported herein was conducted at the Hydraulic Machinery Laboratory of the California Institute of Technology and was authorized by a letter dated January 17, 1944 from Dr. E. H. Colpitts, Chief of Section 6.1, National Defense Research Committee.

As this investigation has developed, it is apparent that a very extensive series of tests will have to be made in order to cover the ground in a satisfactory manner. It was, therefore, thought best to prepare this progress report without further delay so that the results so far obtained might be made available. Other progress reports will be issued from time to time as additional tests are completed.

In this report only the tests of ogive and spherogive noses will be described. A total of about 50 models of these two types of nose shape have been tested, and, it is believed, some interesting and valuable information has been obtained. However, all data in this report must be considered as preliminary only and subject to corrections based on future tests. The work so far done has furnished a fairly comprehensive overall picture of the performance of these two types of nose, even though the test data are rather meager.

In order to obtain consistent results, it has been found necessary to make the models to very close tolerances. All linear dimensions are held within + or - 0.001". Especial care is exercised to be certain that the curves forming the nose are truly tangent and match within 0.0001" or less. The angle of the spherical segment forming the tip of a spherogive nose must be held to within a quarter of a degree as, in some cases, a variation of 1° will cause a change of 15% in the value of the cavitation parameter.

METHOD OF TEST

One of the primary objects of the investigation was to determine the point of incipient cavitation for the various nose shapes. This was done by mounting the model in the High Speed Water Tunnel and observing the first evidence of cavitation as the pressure in the tunnel was lowered. The water velocity during

these tests was, in general, held at a constant value of approximately 60 ft/sec. The cavitation parameter, K, for the point of incipient cavitation, is calculated from the velocity and pressure in the tunnel as described in the Appendix attached hereto. This value of K for incipient cavitation will, hereafter, have the symbol K_i.

After the point of incipient cavitation had been determined, the pressure in the tunnel was lowered, corresponding to decreasing values of the cavitation parameter, and high-speed photographs were taken of the development of the cavitation bubble. These photographs, which furnish valuable data regarding the nature, location, and extent of the cavitation effects for each nose shape, appear throughout the report and are discussed in the text.

OGIVE NOSES

Sixteen ogive nose shapes of different proportions have been investigated. The ogive nose profile is formed by two equal arcs tangent to the cylindrical portion of the projectile and meeting at a point. Figure 1 is a drawing of the family of 16 ogive noses that were tested. The radii of these ogives varied from 0.5 to 8.12 calibers, a caliber being the maximum diameter of the projectile.

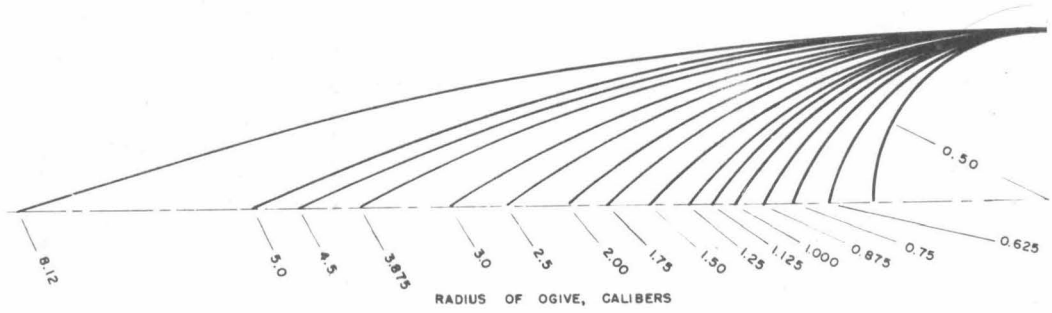

FAMILY OF OGIVES

FIGURE 1

In Table A are given the observed values of K for incipient cavitation for the ogive noses, and these values are plotted in Figure 2. From the smooth curve in Figure 2, the value of K_i for each ogive has been determined and these are shown in Table A. These latter values are the ones that will be referred to throughout this report as the K for incipient cavitation for ogive noses. The values of K_i can also be plotted against the Curvature (1/radius) of the ogive. Figure 3 shows this curve in which the values of K_i have been taken from the smooth curve of Figure 2.

TABLE A

Incipient Cavitation Parameter, K_i, for Ogive Noses

Ogive Radius Calibers	Curvature = 1/Rad Calibers	Observed K_i	K_i from Curve-Fig.3
0.5	2.0	0.75	0.75
0.625	1.60	0.61	0.60
0.75	1.33	0.53	0.52
0.875	1.14	0.46	0.46
1.0	1.00	0.40	0.43
1.125	0.89	0.40	0.41
1.25	0.80	0.39	0.39
1.50	0.67	0.37	0.37
1.75	0.57	0.37	0.35
2.0	0.50	0.34	0.33
2.5	0.40	0.31	0.30
3.0	0.33	0.27	0.28
3.875	0.26	0.26	0.25
4.5	0.22	0.21	0.24
5.0	0.20	0.21	0.22
8.12	0.12	0.17	0.17

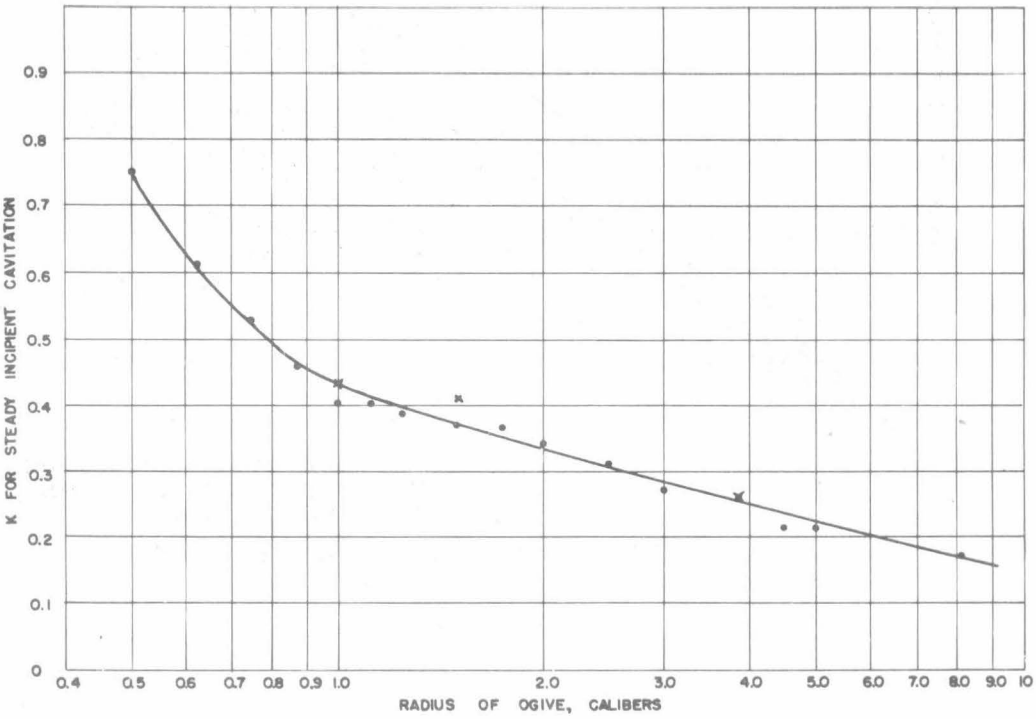

OGIVE RADIUS VS. CAVITATION PARAMETER

FIGURE 2

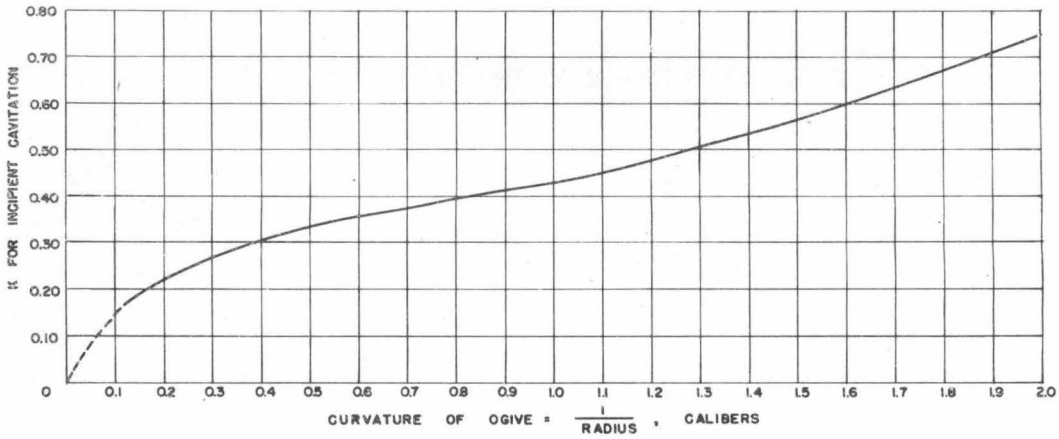

CAVITATION PARAMETER VS. CURVATURE. OGIVE NOSES

FIGURE 3

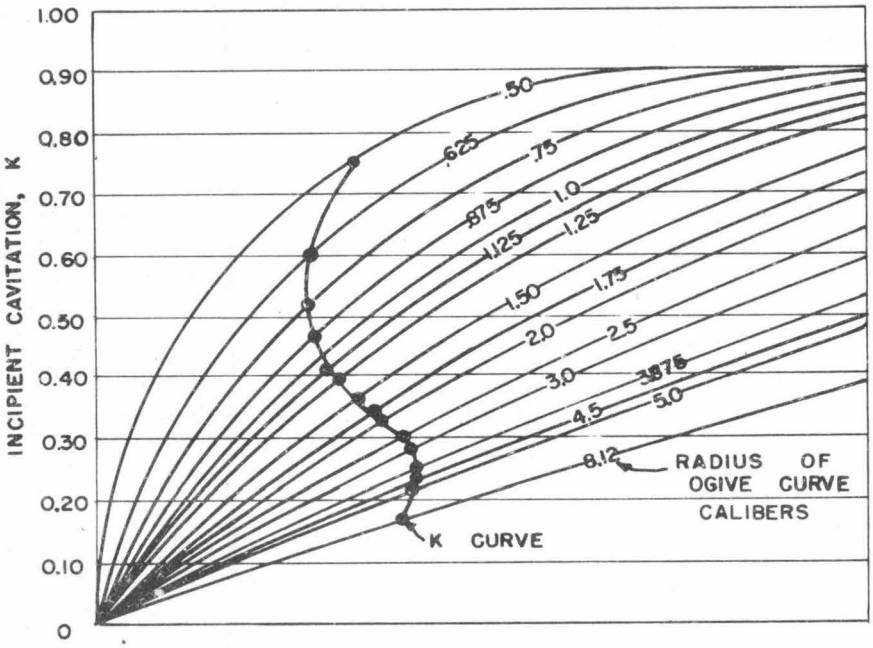

INTERSECTION OF OGIVE CURVE WITH K CURVE GIVES K FOR INCIPIENT CAVITATION.

CAVITATION PARAMETER VS. NOSE SHAPE
OGIVE NOSES
FIGURE 4

In Figure 4 the value of K_i is plotted on its corresponding ogive profile. This gives a more graphic indication of the variation of K_i with ogive radius.

The curve in Figure 2 indicates that there is a rapid decrease in K for incipient cavitation, as the ogive radius increases from 0.5 caliber (the hemisphere) to about 1.0 caliber and from this point the value of K_i is much less affected by an increase in the radius.

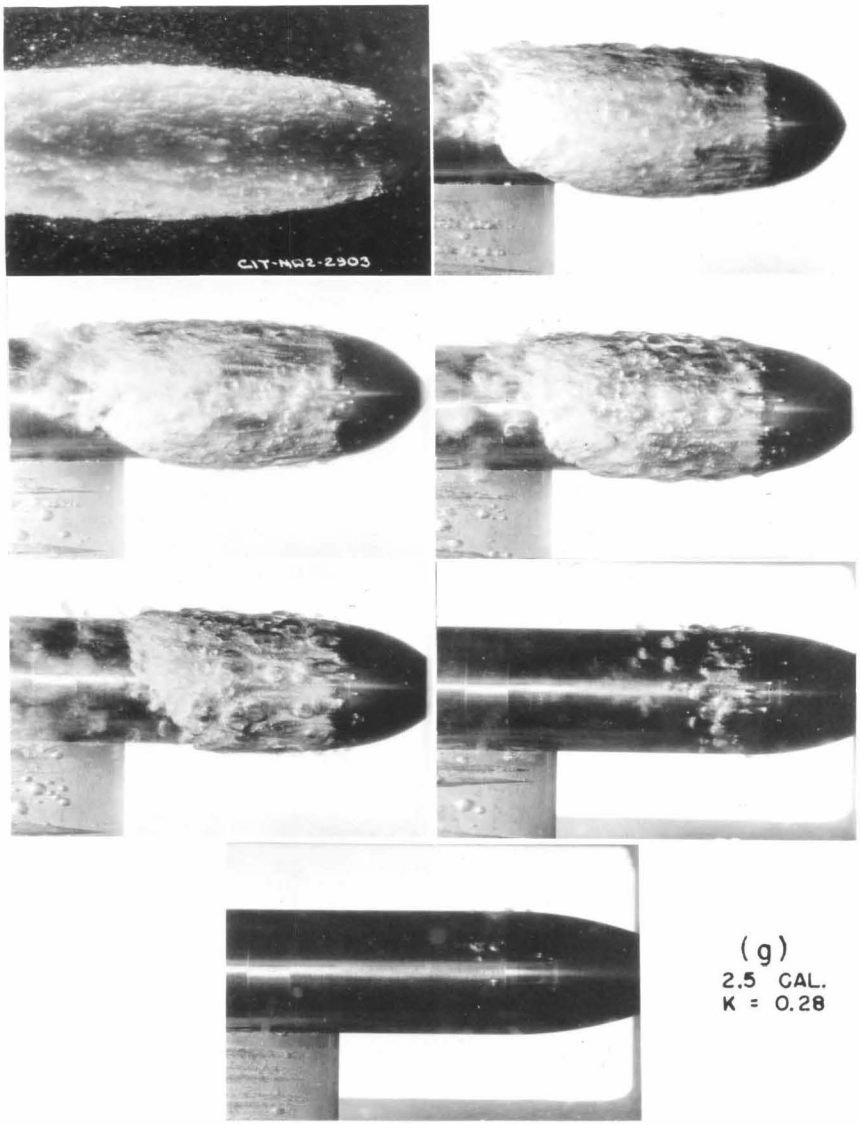

(a)
0.5 CAL.
K = 0.24

(b)
0.625 CAL.
K = 0.28

(c)
0.75 CAL.
K = 0.27

(d)
0.875 CAL.
K = 0.26

(e)
1.0 CAL.
K = 0.26

(f)
1.75 CAL.
K = 0.27

(g)
2.5 CAL.
K = 0.28

CAVITATION BUBBLES
OGIVE NOSES

K APPROX. 0.26

FIGURE 5

OGIVE CAVITATION PHOTOGRAPHS

The series of photographs in Figure 5 shows how the size of the cavitation bubble varies with different ogive shapes. These were selected to have practically the same value of K so the change in bubble size is due almost entirely to the nose shape. As would be expected, the more blunt the nose, the greater the cavitation effect.

Figure 6 shows a series of cavitation photographs similar to Figure 5 but for a lower value of K and longer radius ogives. In this series also is seen the decrease in cavitation effect due to decreasing bluntness of the nose.

In Figure 7 is shown the development of the cavitation bubble on a 2.0 caliber ogive as the value of K is reduced from 0.31 to 0.18. As the K for incipient cavitation for this nose is 0.33, the first picture shows about the least amount of cavitation bubble that can be photographed. In the last picture the bubble is quite well developed, although it has not by any means reached the proportions of a "full bubble". These pictures illustrate what has been termed "coarse-grained cavitation", in which the cavitation bubble as a whole is made up of a multiplicity of fairly large individual bubbles. It is seen in this series that this formation persists throughout the various degrees of cavitation.

BUBBLE LOCATION

Photographs of the various ogive noses were measured in order to determine the location of the well developed cavitation bubble. Measurements were made from the tip of the nose to the forward edge of the bubble and the results are plotted in Figure 8. With very few exceptions these measurements show a steady increase in the distance from the point of tangency of the ogive curve and the cylinder, to the forward edge of the bubble as the ogive radius increases. Measurements of the angle between the axis of the nose and the radius drawn to the forward edge of the bubble showed that this remained practically constant at 86°. The measured values of this angle are plotted in Figure 9.

HEMISPERICAL NOSE

The hemispherical nose is the limiting case of an ogive nose with minimum radius. It is interesting to compare the development of the bubble on this nose with that of the 2.0 caliber ogive just discussed. Figure 10 shows the development of cavitation on a hemispherical nose with values of K ranging from 0.68 to 0.21, incipient cavitation on this nose occurring at a value of $K_i = 0.75$. In this series of pictures it is seen that the cavitation bubble is of a different type, being termed "fine-grained cavitation". The cavitation effect commences as a band of very fine bubbles having a homogenous appearance which form persists throughout the development of the bubble proper.

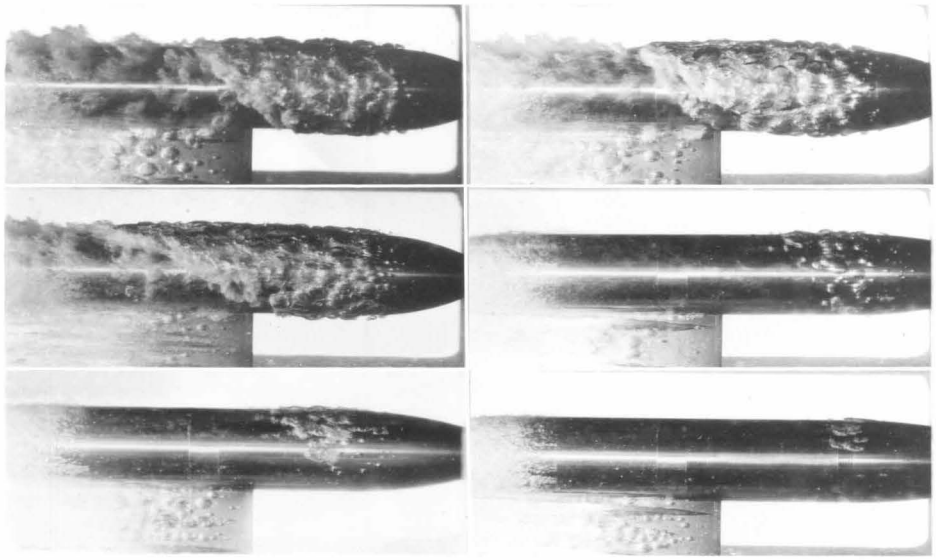

CAVITATION BUBBLES
OGIVE NOSES
K APPROX. 0.19

FIGURE 6

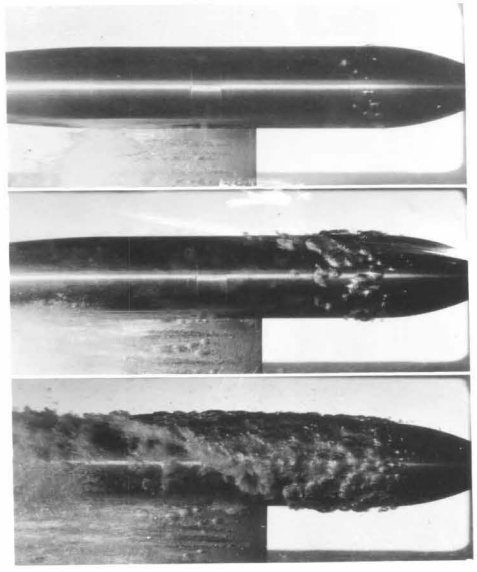

DEVELOPMENT OF BUBBLE
2.0 CAL. OGIVE

FIGURE 7

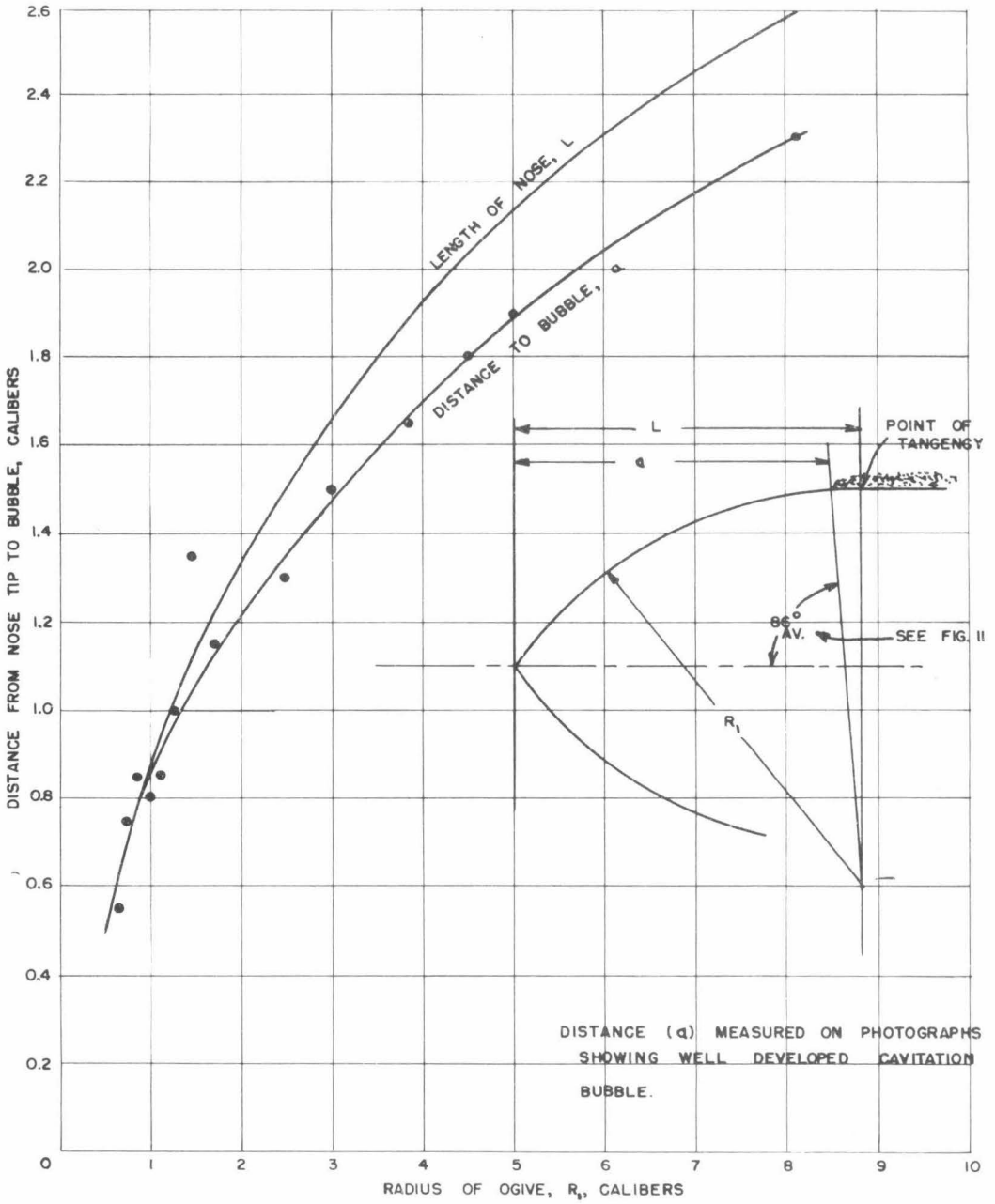

DISTANCE OF CAVITATION FROM TIP OF NOSE

FIGURE 8

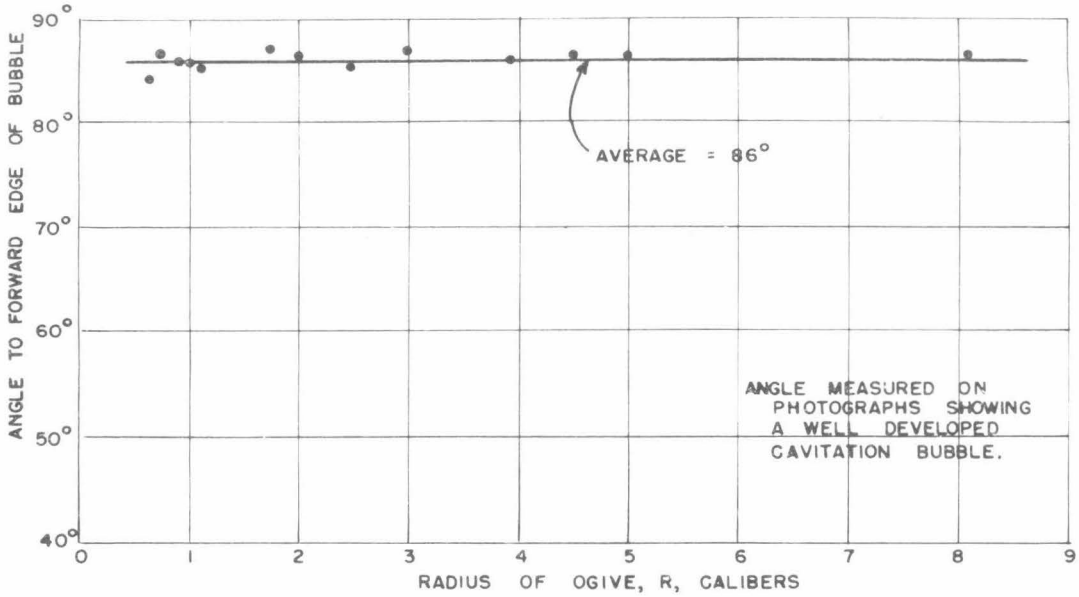

ANGLE TO FORWARD EDGE OF CAVITATION BUBBLE
OGIVE NOSES

FIGURE 9

TRANSITION ZONE

It has already been pointed out that the curve of K for incipient cavitation plotted against ogive radius shows a rather abrupt change in slope in the region of 1.0 caliber radius. It is interesting and probably significant to note that the type of cavitation bubble also undergoes a change in this region. Noses of less than 1.0 caliber radius show a distinct "fine-grained" cavitation bubble, and those of greater radii than 1.0 caliber have a "coarse-grained" bubble.

Figure 11 shows pictures of three ogive noses having radii of 0.875, 1.00, and 1.125 calibers at three stages of cavitation, roughly for K's of 0.40, 0.33, and 0.26. In the 0.875 series, (a), (b), and (c), it is seen that the cavitation is of the "fine-grained" nature throughout, although some of the "coarse-grained" bubbles are appearing at the lowest value of K. The 1.0 caliber series (d), (e), and (f), shows the typical "fine-grained" cavitation band at the highest value of K, (d), and somewhat of a mixture of "fine and coarse grain" in (e) and (f). The 1.125 caliber series, (g), (h), and (i), shows the typical "coarse grain" throughout.

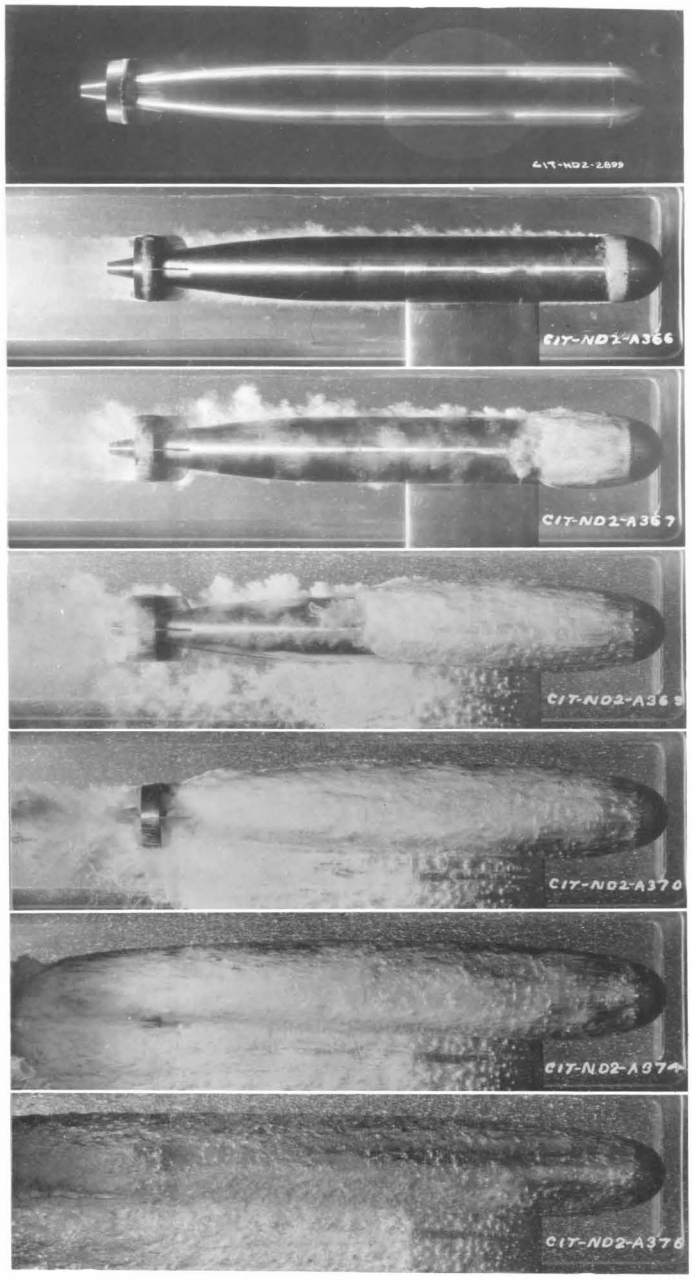

(a)
K = 0.71

(b)
K = 0.54

(c)
K = 0.35

(d)
K = 0.24

(e)
K = 0.22

(f)
K = 0.21

(g)
K = 0.21-

DEVELOPMENT OF BUBBLE
HEMISPHERICAL NOSE

FIGURE 10

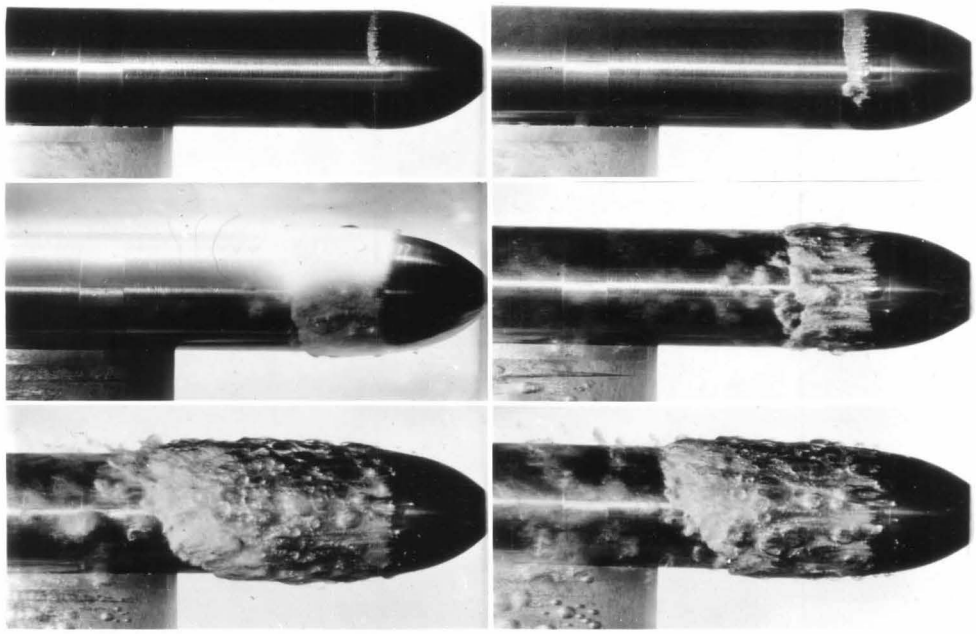

(a) K = 0.43

(b) K = 0.34

(c) K = 0.26

(d) K = 0.38

(e) K = 0.33

(f) K = 0.26

0.875 CAL. OGIVE

1.00 CAL. OGIVE

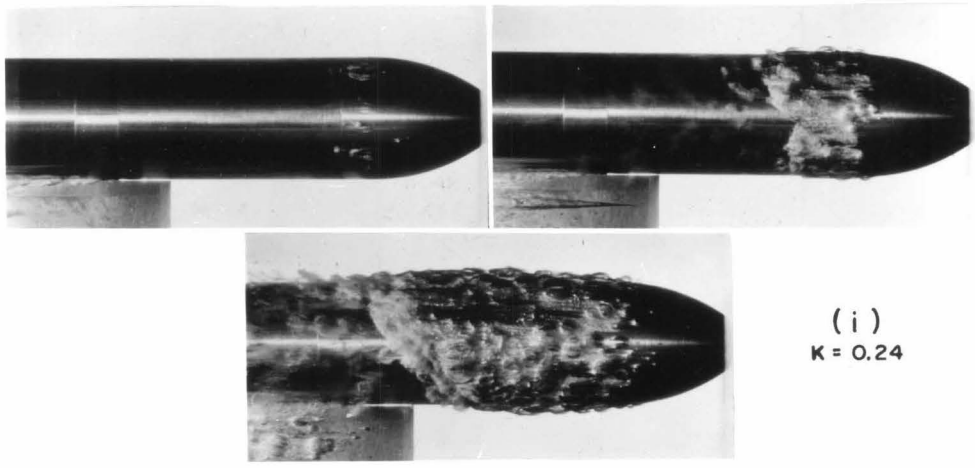

(g) K = 0.40

(h) K = 0.32

(i) K = 0.24

1.125 CAL. OGIVE

TRANSITION IN TYPE OF BUBBLE
OGIVE NOSES

FIGURE 11

EFFECT OF YAW

It is intended to investigate the effect of yaw on the cavitation bubble for the full range of noses included in this series. To date, however, results can be reported for the hemispherical nose only. Observations of the value of K for incipient cavitation were made at yaws of 0°, 3°, and 6°, and these results are shown in Figure 12. It is seen that there is a rapid increase in K_i with increasing yaw angle. The significance of this is made more apparent by the scale on the right of the diagram which gives the submergence necessary to avoid cavitation, with this hemispherical nose at a speed of 40 knots. With zero yaw, at 40 knots, cavitation will be avoided with a submergence of 20 feet, but the submergence will have to be increased to 25 feet should the yaw be 3° and with a yaw of 6°, cavitation could not be avoided at any submergence less than 37 feet. Of course, as the speed is increased or decreased, the submergence would have to be increased or decreased accordingly.

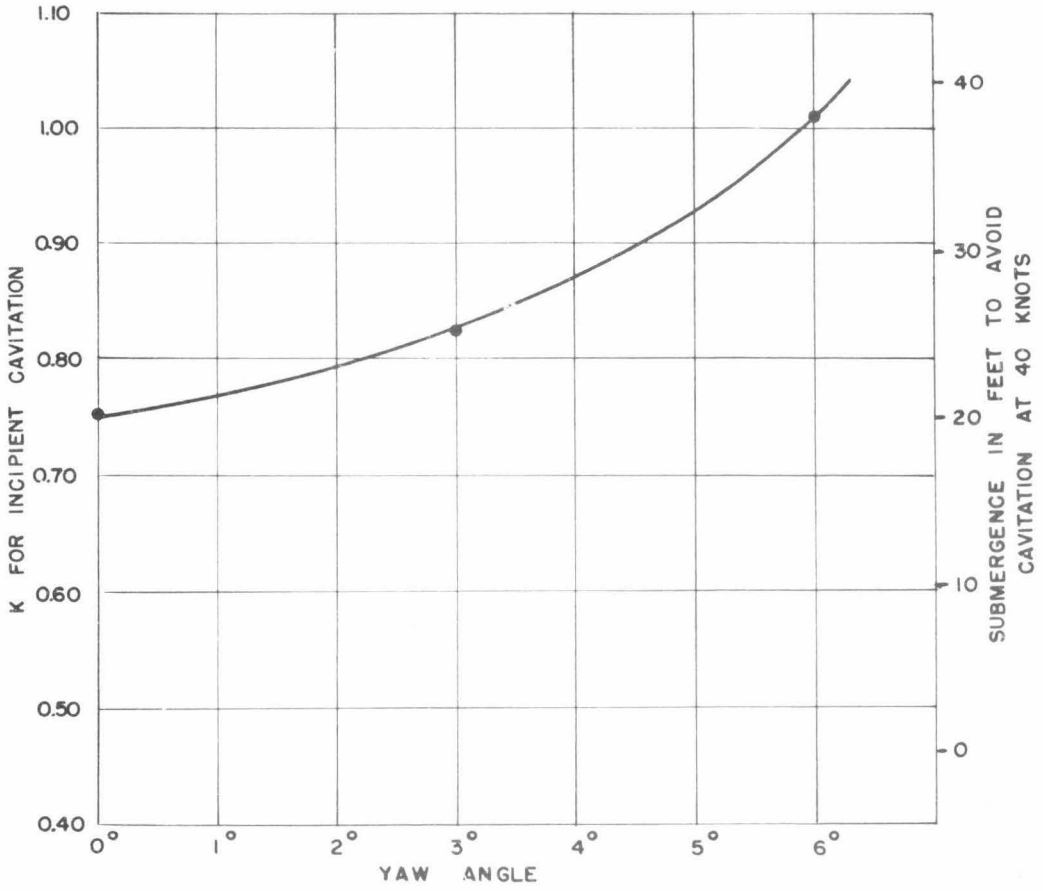

CAVITATION PARAMETER VS. YAW
HEMISPHERICAL NOSE

FIGURE 12

(a)

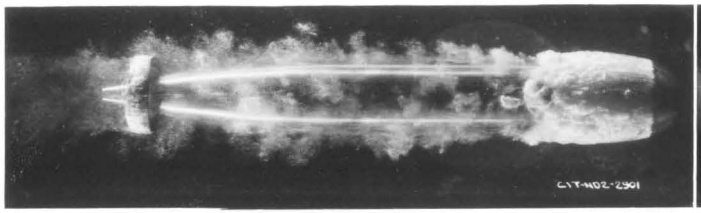

(d)

K = 0.35 YAW = 0° K = 0.22

(b)

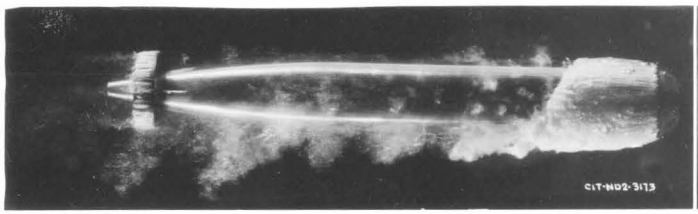

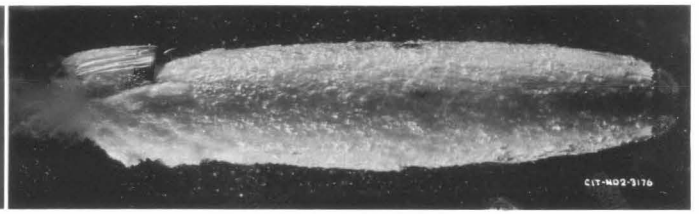

(e)

K = 0.35 YAW = 3° K = 0.23

(c)

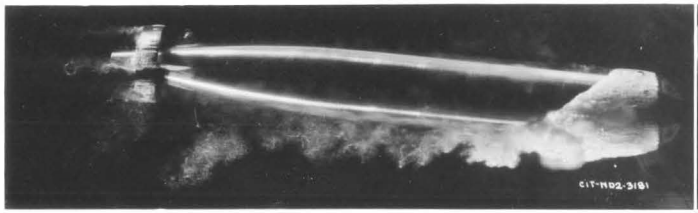

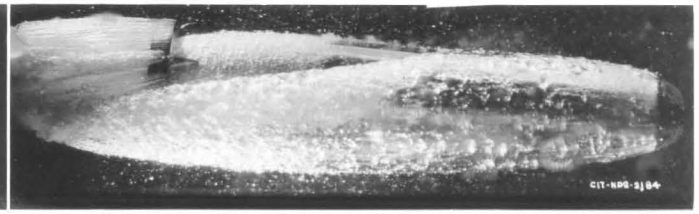

(f)

K = 0.38 YAW = 6° K = 0.23

EFFECT OF YAW ON BUBBLE
HEMISPHERICAL NOSE

FIGURE 13

Figure 13 shows photographs of the hemispherical nose at yaws of 0°, 3°, and 6°, each for two different values of K. These pictures show clearly the effect of yaw on the shape and position of the cavitation bubble. They also show quite conclusively that the plane of the forward edge of the cavitation bubble remains practically at right angles to the direction of travel regardless of the yaw, at least for yaw angles up to 6°. This is considered one of the inherent properties of the spherical nose tip.

SPHEROGIVE NOSES

Thirty-five spherogive noses of various proportions have been tested thus far. The tests on this number of noses have furnished interesting and instructive data but not by any means sufficient to predict definitely the performance of any given spherogive nose. As before stated, it is believed that enough information is now available to enable some general conclusions to be drawn regarding the properties of the spherogive family of noses, but much yet remains to be done.

A spherogive nose shape is made by terminating an ogive in a segment of a sphere, the curves of the sphere and ogive, of course, being tangent at their junction. Figure 14 shows that a family of spherogives can be constructed in three ways: (a) by maintaining the radius of the ogive (R_1) constant, which gives a series of spheres of varying radii (R_2) and also varying half-sphere angles (θ); (b) by maintaining the half-sphere angle (θ) constant, resulting in varying values for the radii of both the sphere and ogive; (c) by maintaining the radius of the sphere (R_2) constant which results in varying values for the radius of the ogive and the half-sphere angle. Some interesting tests of families of noses constructed in this manner will be discussed.

The program contemplated tests on five families of spherogives based on ogives having radii of 5.0, 3.5, 2.3, 1.5, and 1.0 calibers. Only a few models were made for the 3.5 and 1.5 caliber series and the test results on these were not very consistent so emphasis will be placed mainly on the 5.0, 2.3, and 1.0 caliber series. Figure 15 shows profiles of these three families of spherogives drawn to scale so their relative shapes can be easily observed. Table B gives the observed values of K for incipient cavitation for the spherogive nose shapes tested.

These values of K_i have been plotted against the half-sphere angle (θ) for each nose and faired curves drawn through the points as shown in Figures 16 to 20 inclusive. Figure 21 combines all of the K_i vs θ curves in one chart and from this some interesting observations can be made. The horizontal portions of the curves represent the incipient cavitation parameter for the ogive alone, corresponding to those given by the curve in Figure 2. This shows that the sphere can be increased in size without affecting the incipient cavitation parameter until some critical value of the half-sphere angle is reached. This region is represented by the shaded zone at the break in the curves. This shaded region

represents a transition from cavitation on the ogive to cavitation on the sphere. In other words, all nose shapes represented by the curves in the region above the shaded zone will cavitate first on the sphere and all below this zone will cavitate first on the ogive. The line of demarcation is not definite, for, as might be expected, cavitation can occur on the ogive and on the sphere simultaneously.

TABLE B

Incipient Cavitation Parameter, K_i, for Spherogive Noses

Ogive Rad. R_1	Half-Sphere Angle θ^o	Observed K_i	K_i for Ogive only
5.0	70	.22	.22
"	72	.22	
"	73	.26	
"	74	.27	
"	76	.35	
"	78	.44	
"	81	.54	
"	84	.59	
"	86	.63	
3.5	74	.33	.26
"	77	.45	
"	80	.54	
2.3	69	.33	.32
"	71	.35	
"	72	.35	
"	74	.40	
"	76	.45	
"	78	.50	
"	80-1/2	.58	
1.5	72	.46	.37
"	74	.47	
"	76	.55	
"	78	.54	
1.0	63	.49	.43
"	65	.51	
"	67	.49	
"	70	.52	
"	72	.53	
"	74	.55	
"	76	.60	
"	78	.63	

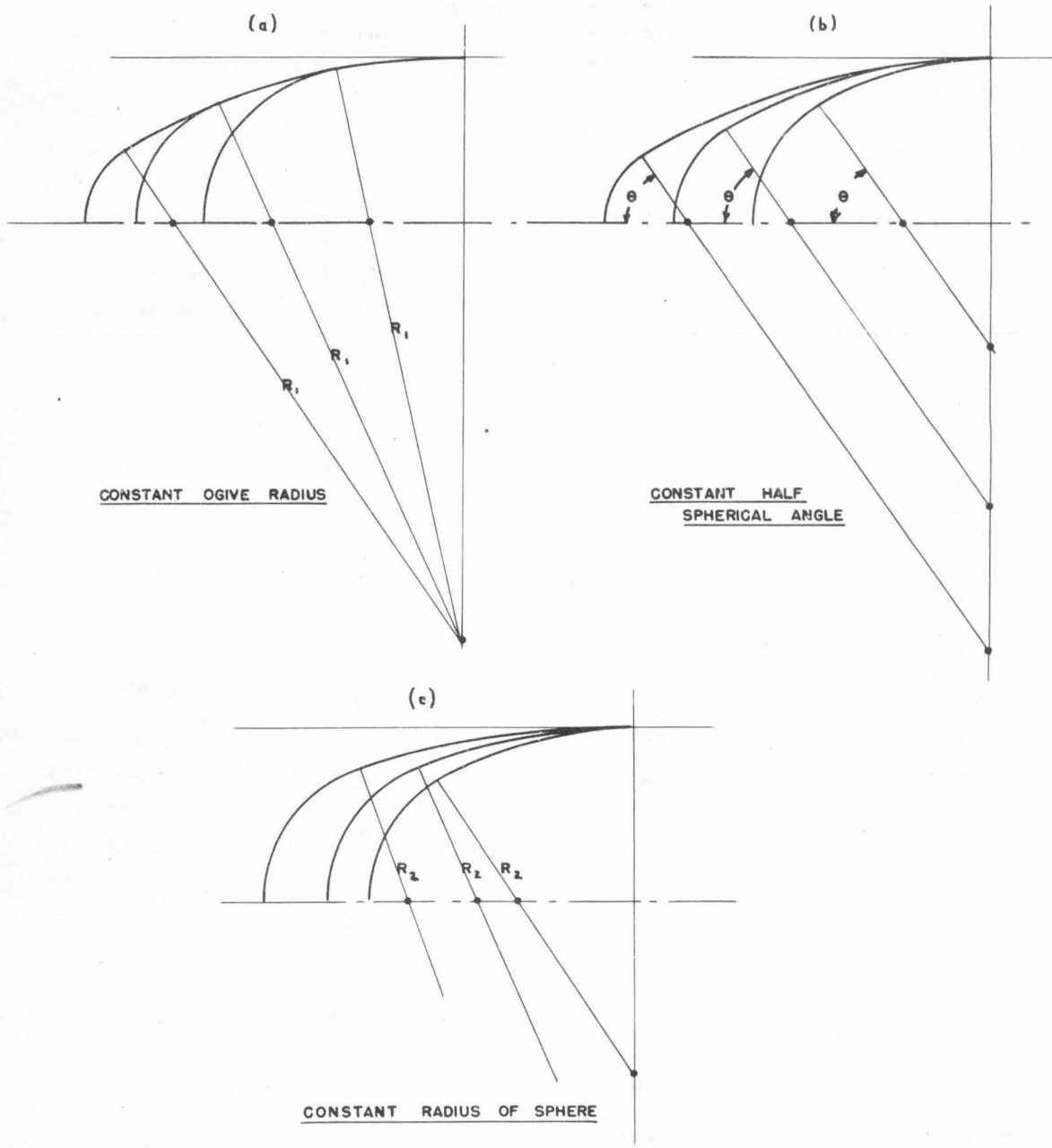

METHOD OF CONSTRUCTION
FAMILIES OF SPHEROGIVES

FIGURE 14

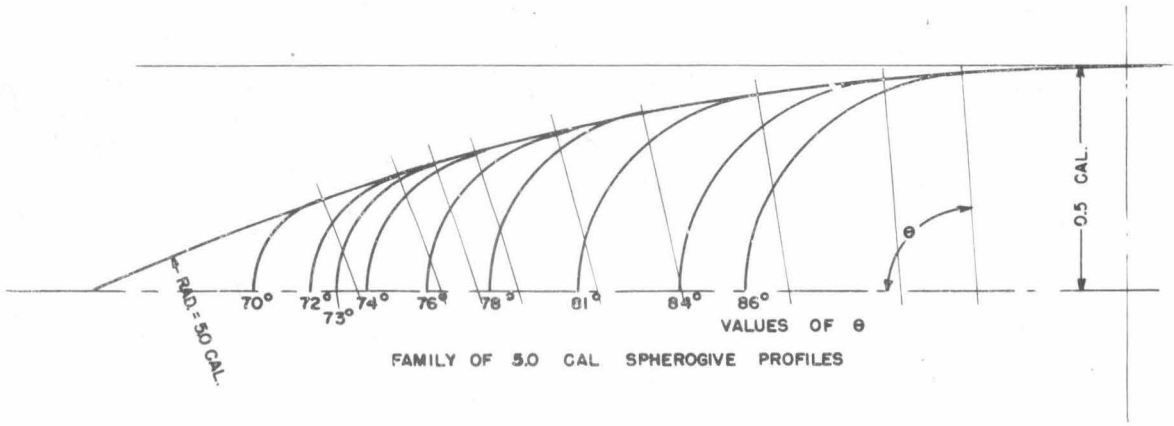

FAMILY OF 5.0 CAL SPHEROGIVE PROFILES

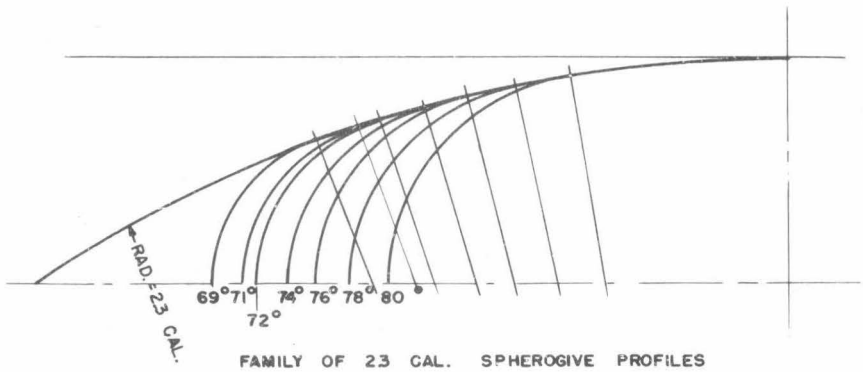

FAMILY OF 2.3 CAL. SPHEROGIVE PROFILES

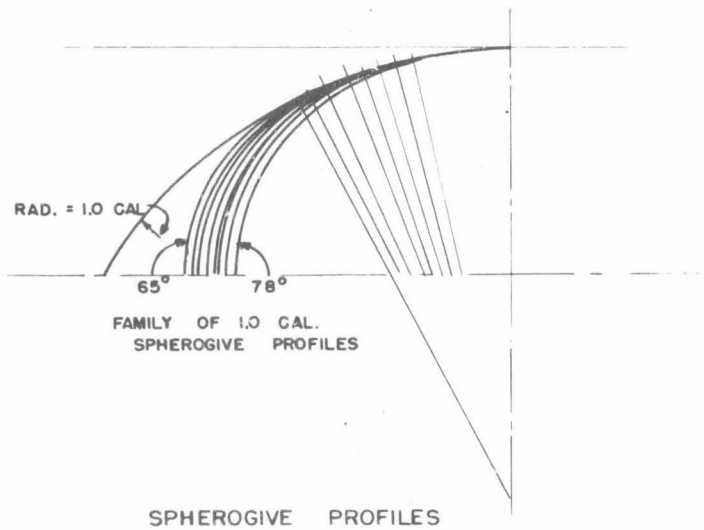

FAMILY OF 1.0 CAL.
SPHEROGIVE PROFILES

SPHEROGIVE PROFILES

FIGURE 15

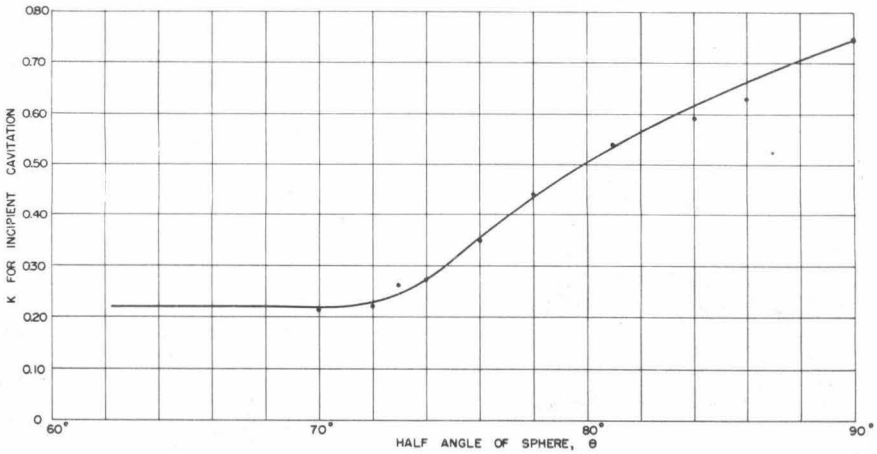

SPHERE ANGLE VS. CAVITATION PARAMETER
5.0 CAL. SPHEROGIVE

FIGURE 16

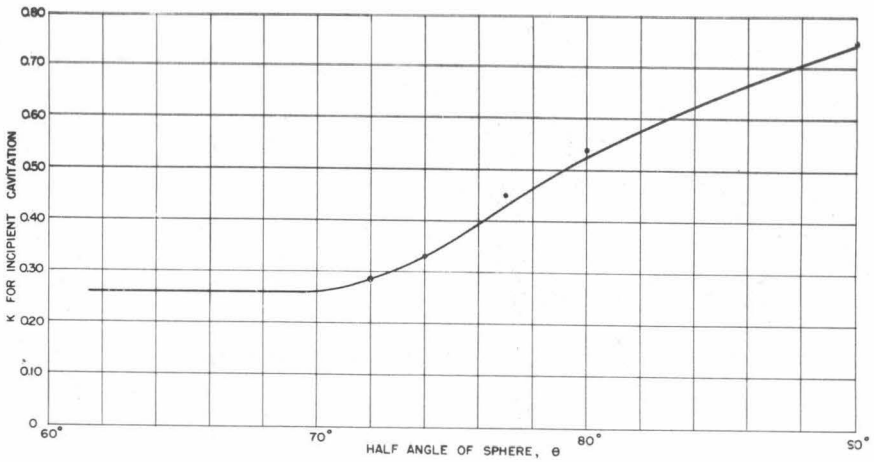

SPHERE ANGLE VS. CAVITATION PARAMETER
3.5 CAL. SPHEROGIVE

FIGURE 17

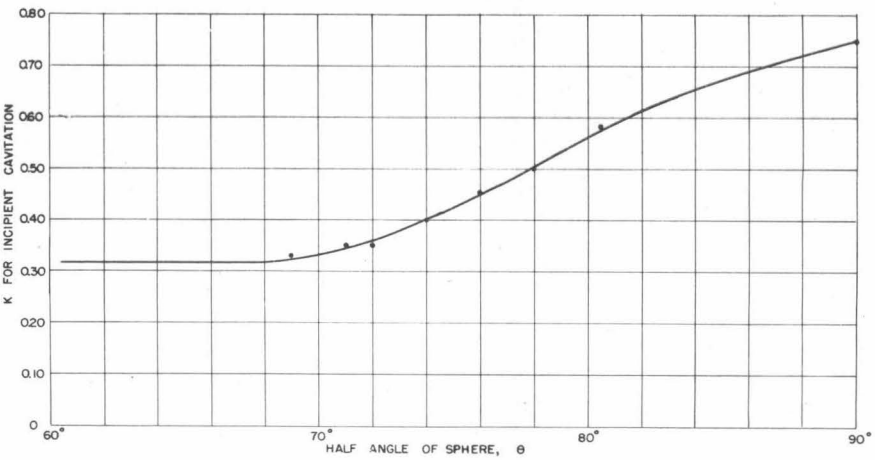

SPHERE ANGLE VS. CAVITATION PARAMETER
2.3 CAL. SPHEROGIVE

FIGURE 18

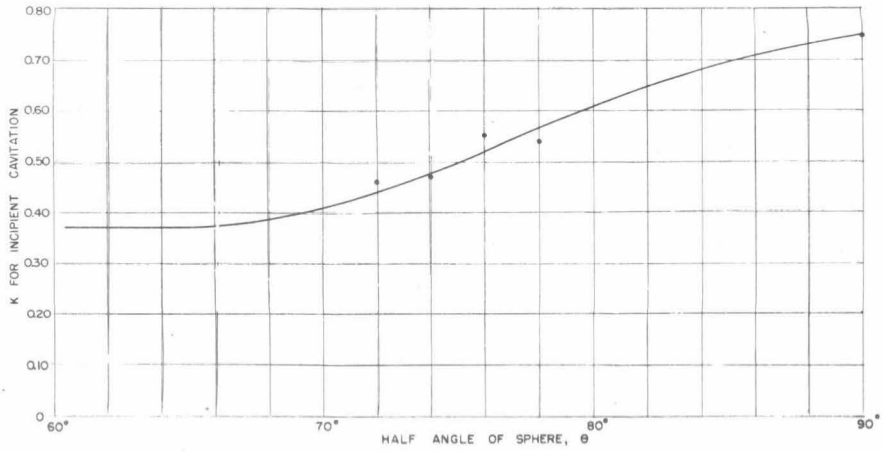

SPHERE ANGLE VS. CAVITATION PARAMETER
1.5 CAL. SPHEROGIVE

FIGURE 19

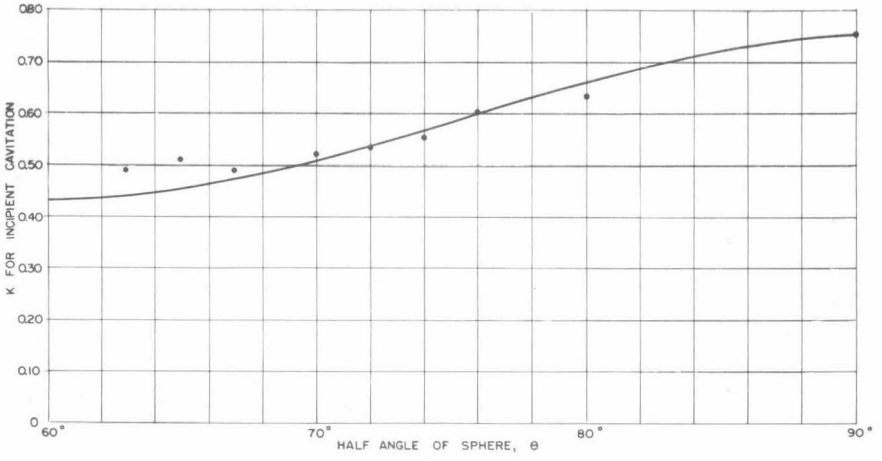

SPHERE ANGLE VS. CAVITATION PARAMETER
1.0 CAL. SPHEROGIVE

FIGURE 20

Figure 21 makes possible the design of spherogive noses to fit varying requirements for bluntness and incipient cavitation.

The data given in Figure 21 make possible the plotting of another chart showing the relation between the radii of the sphere and ogive, the half angle of the sphere and the cavitation parameter. This chart appears as Figure 22 and covers the whole field of possible spherogives, although available data permits the plotting of only a portion of the curves involved. As will be seen, this chart gives the radius of the sphere corresponding to any half-sphere angle and several values of ogive radius. In addition, there appear dotted lines of constant K values for incipient cavitation. The shaded zone is similar to that in Figure 21 in that it represents the region of transition from cavitation on the ogive to cavitation on the sphere.

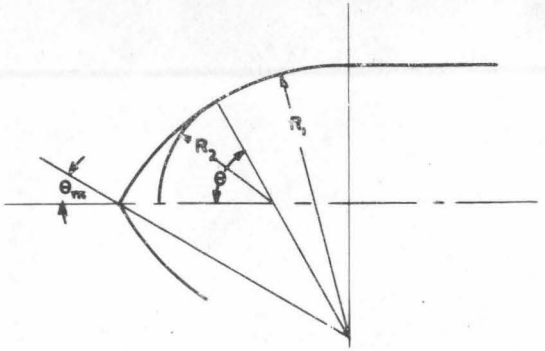

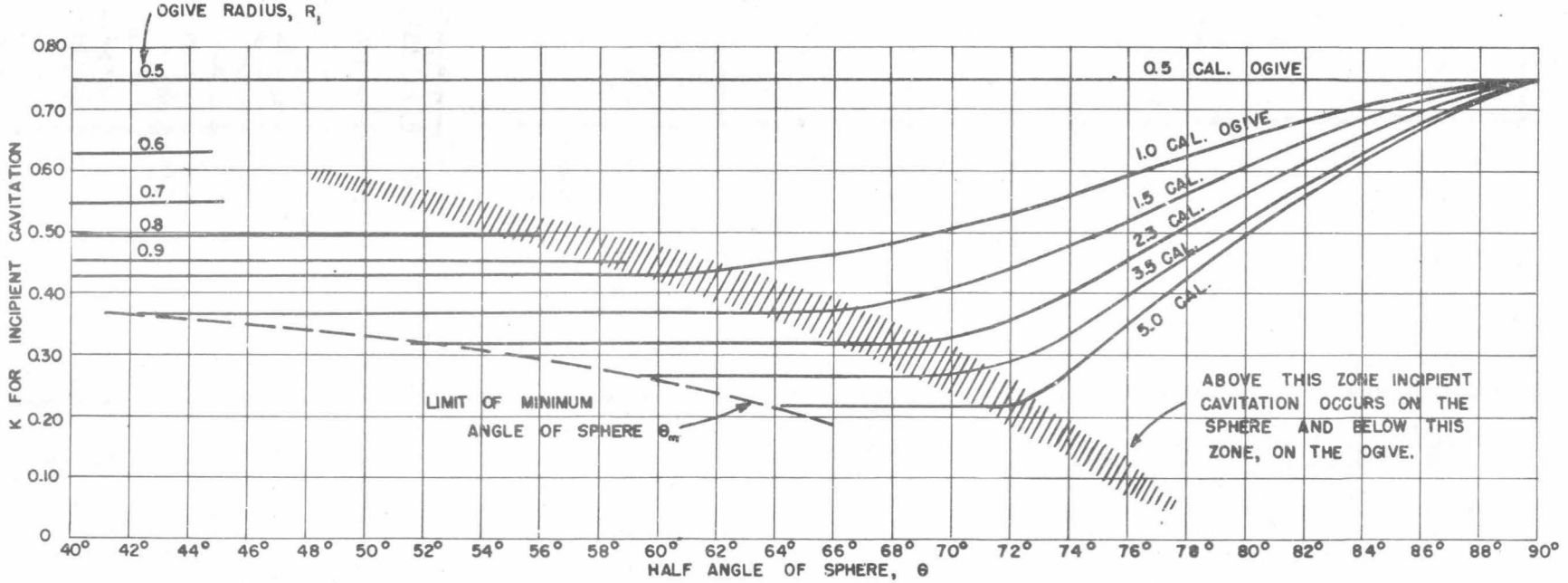

SPHERE ANGLE VS. CAVITATION PARAMETER
SPHEROGIVE NOSES

FIGURE 21

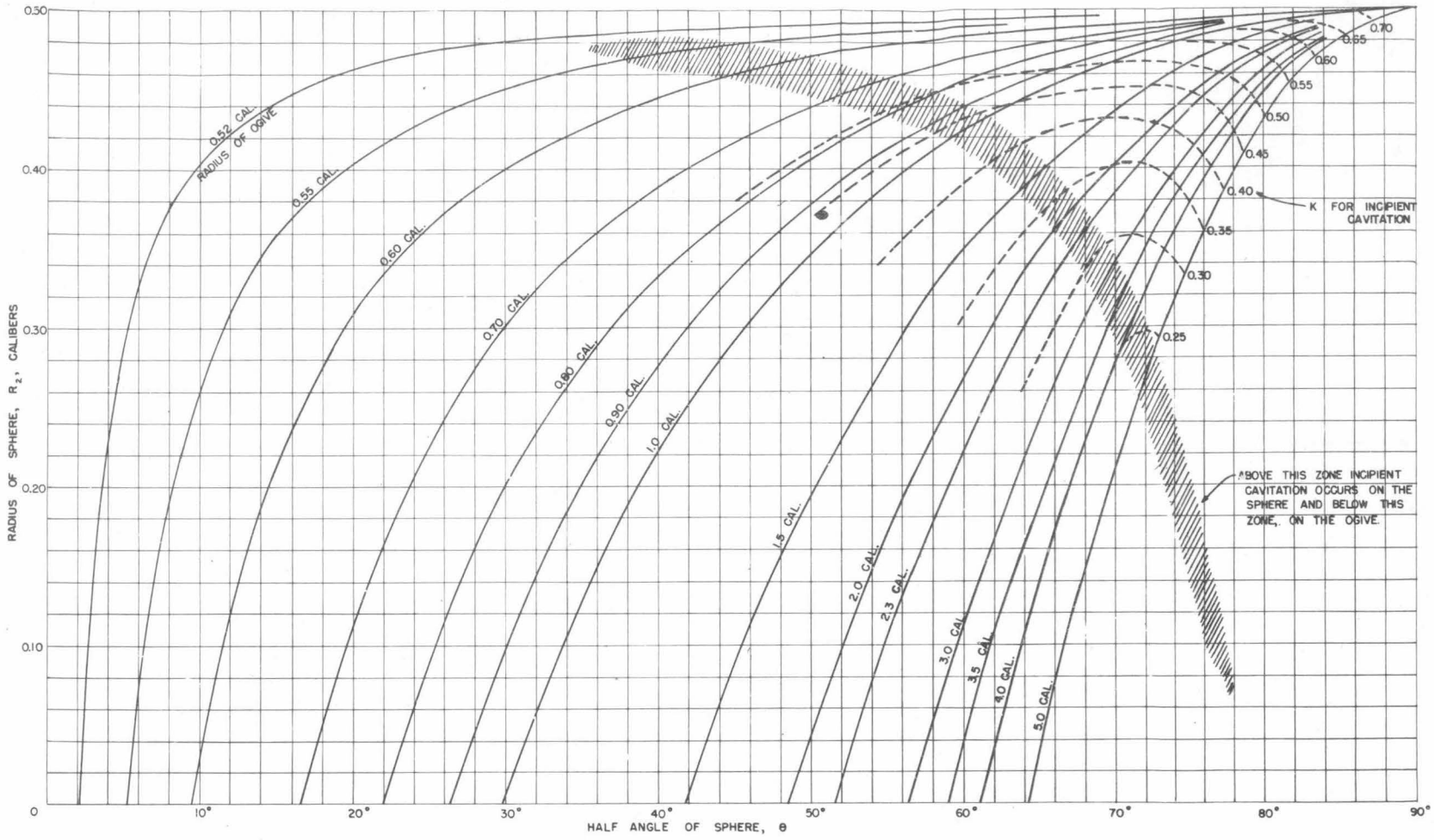

RELATION BETWEEN
RADIUS OF SPHERE, RADIUS OF OGIVE, HALF ANGLE
OF SPHERE AND CAVITATION PARAMETER

FIGURE 22

An inspection of Figure 22 shows a surprisingly small region in which the cavitation is governed by the sphere. It also shows that the longer the ogive radius, the larger the half-sphere angle can be without increasing the incipient cavitation parameter. The shaded zone representing the region of transition from cavitation on the ogive to cavitation on the sphere appears to intercept the horizontal axis at about 80° half-sphere angle, indicating that cavitation will always be on the sphere for angles above 80° regardless of the ogive radius.

BUBBLE DIAMETER

An attempt was made to determine the effect of the radius of the sphere on the maximum diameter of the full cavitation bubble. Photographs of the 1.0, 2.3, and 5.0 caliber spherogive noses under full cavitation were carefully measured and the bubble diameter, in calibers, obtained. In the entire group of noses measured the sphere radius varied from a minimum of 0.211 calibers to 0.500 calibers, the maximum for the hemisphere.

In Figure 23 the maximum bubble diameter has been plotted against the radius of the sphere, both in calibers. It is remarkable to note that there appears to be a linear relationship between these two quantities, although it must be remembered that the measurement of these small photographs is subject to many errors.

The 5.0 caliber series is the only one in which it was possible to make measurements of the bubble diameter for values of the sphere radius in the region where cavitation occurred on the ogive only. There are two noses with sphere radii of 0.211 and 0.268 calibers which have the same bubble diameter. This is not unexpected as this is the bubble diameter for the ogive, the sphere having no effect. The dotted horizontal lines indicating the bubble diameters for 2.3 and 1.0 caliber ogives are assumptions, although they are believed to be fairly accurate as they are drawn to correspond approximately to the bubble diameters for noses close to the transition point. No photographs have been taken of the full bubbles produced by ogive noses, so the diameters of these could not be determined by measurement.

Figure 23 furnishes good evidence to support the theory advanced by Dr. R. T. Knapp that the full bubble diameter is determined by the sphere radius. See Report No. 6.1-sr207-1900 entitled, "Entrance and Cavitation Bubbles" by Dr. R. T. Knapp.

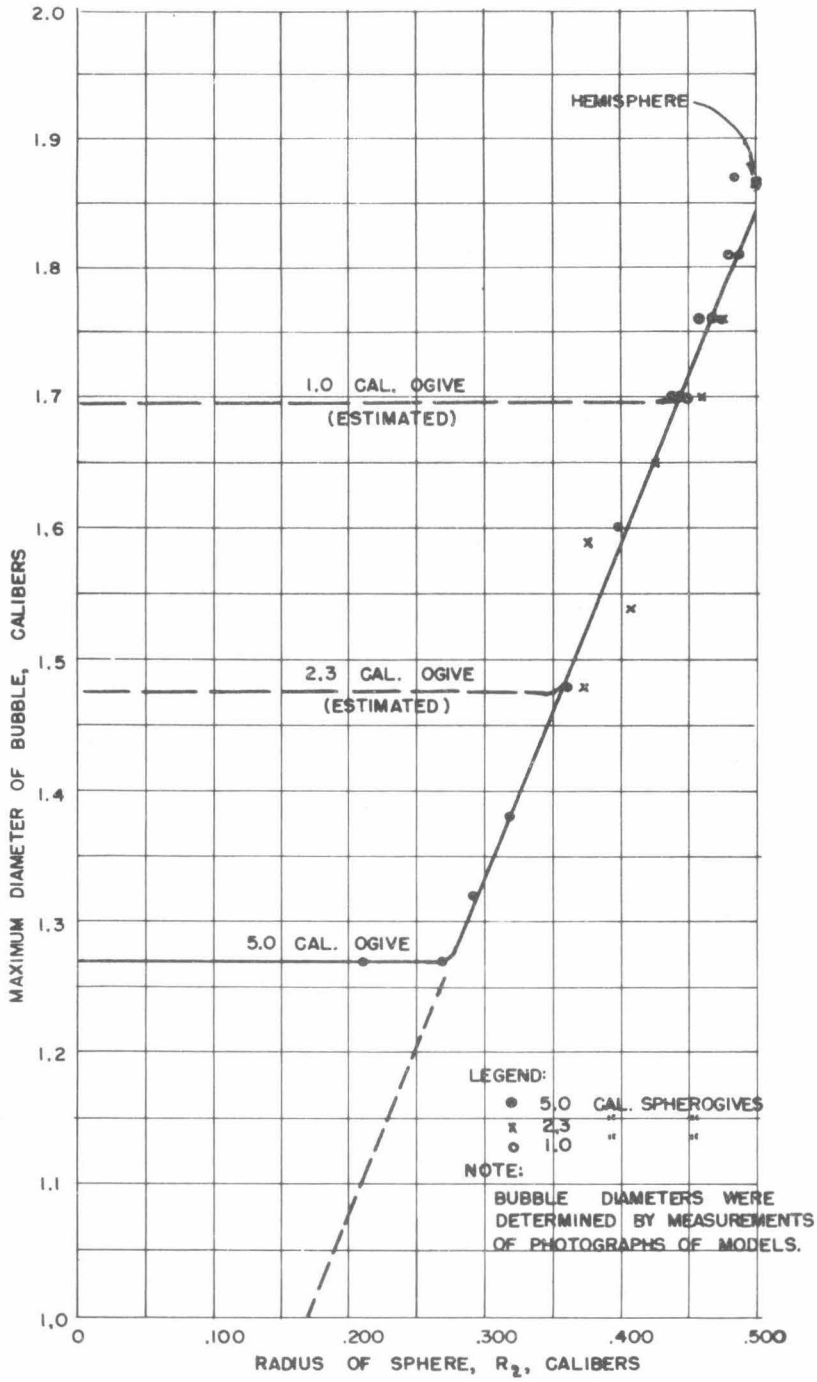

RADIUS OF SPHERE VS. BUBBLE DIAMETER
SPHEROGIVE NOSES

FIGURE 23

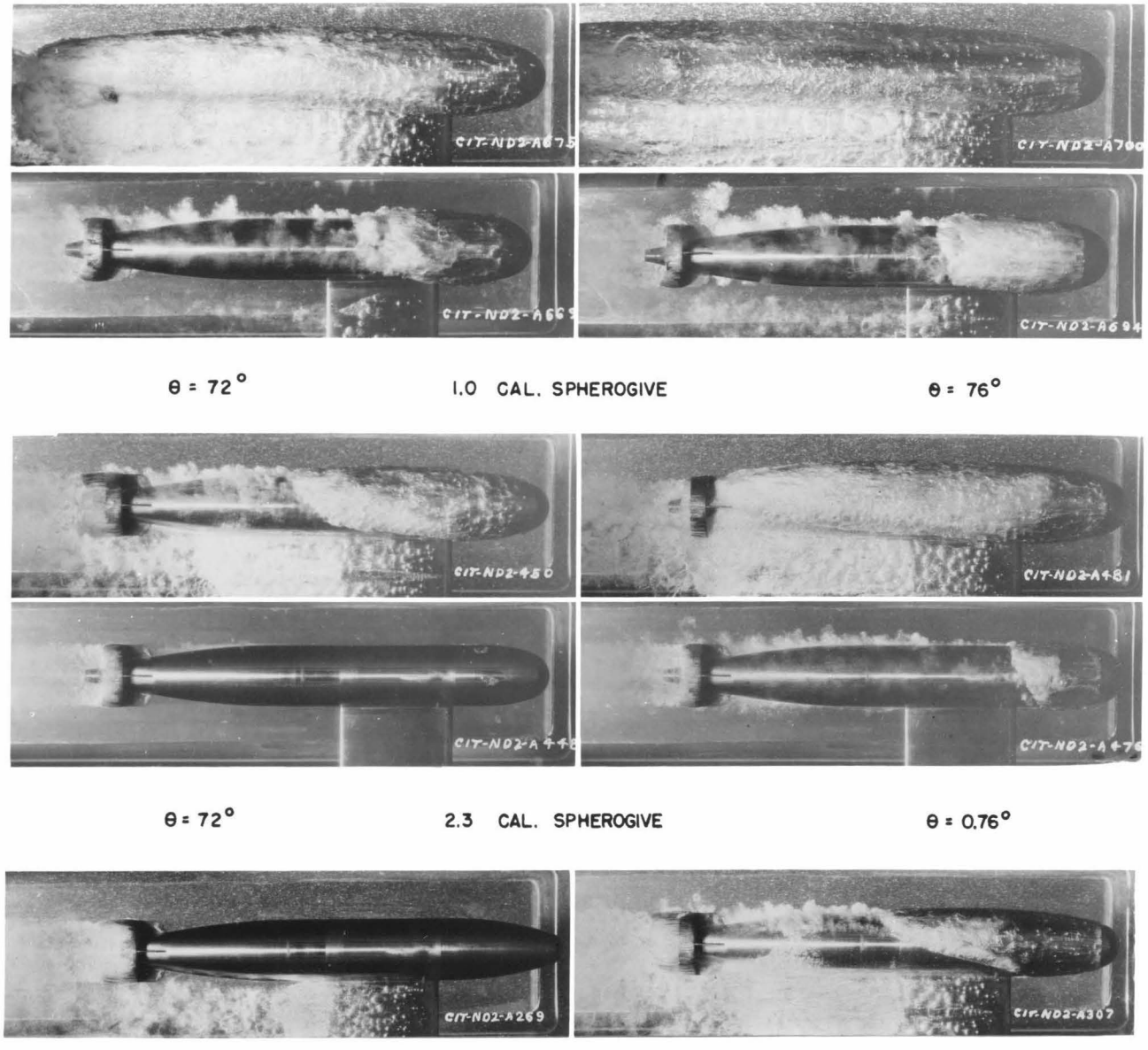

EFFECT OF SIZE OF SPHERE ON CAVITATION PARAMETER
SPHEROGIVE NOSES

FIGURE 24

EFFECT OF THE SPHERE SIZE

It has been shown that the full bubble diameter is determined by the radius of the sphere. The curves in Figure 21 show that incipient cavitation is governed by the half angle of the sphere (θ) for a given ogive. It is also true that the half angle of the sphere determines the extent and nature of the cavitation bubble during its development after the point of incipient cavitation has been passed. In Figure 24 have been assembled photographs of cavitation effects on spherogive noses having ogive radii of 1.0, 2.3, and 5.0 calibers and half-sphere angles of 72° and 76°.

Comparing Photographs (a) and (f) of the 1.0 caliber series for a K of 0.21, it is seen that increasing the half-sphere angle (θ) from 72° to 76° greatly increases the size of the cavitation bubble. The 72° sphere produces a bubble only slightly longer than the projectile, whereas the 76° sphere produces practically a full cavitation bubble. A comparison of (b) and (g) for a higher value of K shows a decided increase in the extent of the bubble for the larger sphere angle. A like comparison can be made with the photographs of the 2.3 caliber and 5.0 caliber series; in every case there is a pronounced increase in the cavitation effect due to increasing the half-sphere angle with the cavitation parameter remaining constant.

In connection with Figure 24, it is interesting to note that Photographs (b), (h), (i), and (j) show cavitation on both the sphere and the ogive.

In Figure 25 is shown how the cavitation bubble is affected by variations in the ogive and sphere radii, the half-sphere angle remaining constant. Photographs (a), (b), (c), and (d) show the bubble for four spherogive noses with a half-sphere angle of 72° and K remaining constant at 0.21. It is seen that there is an increase in the size of the cavitation bubble as the nose becomes more and more blunt. The four pictures on the right, (e), (f), (g), and (h) were selected to show approximately the same degree of cavitation, and it should be observed that the value of K, for this condition, increases as the bluntness of the nose increases.

The effect of varying the half-sphere angle is also shown in Figure 26, which is a series of photographs of a family of 5.0 caliber spherogives. In this case the 74° sphere appears to be at the transition point as cavitation is occurring on both the ogive and the sphere. The noses with spherical angles less than 74° cavitate on the ogive and for angles of greater than 74° the cavitation is on the sphere only. The last five photographs have been selected to show approximately the same degree of cavitation and it is seen that as the noses increase in bluntness, i.e., from 76° to 86° for the half-sphere angle, the value of K increases from 0.25 to 0.57. Stating this in terms of submergence and speed, the 76° and 86° noses would have the same degree of cavitation at a speed of 60 knots with a submergence of 57 feet for the 86° nose and only 7 feet for the 76° nose.

CONFIDENTIAL

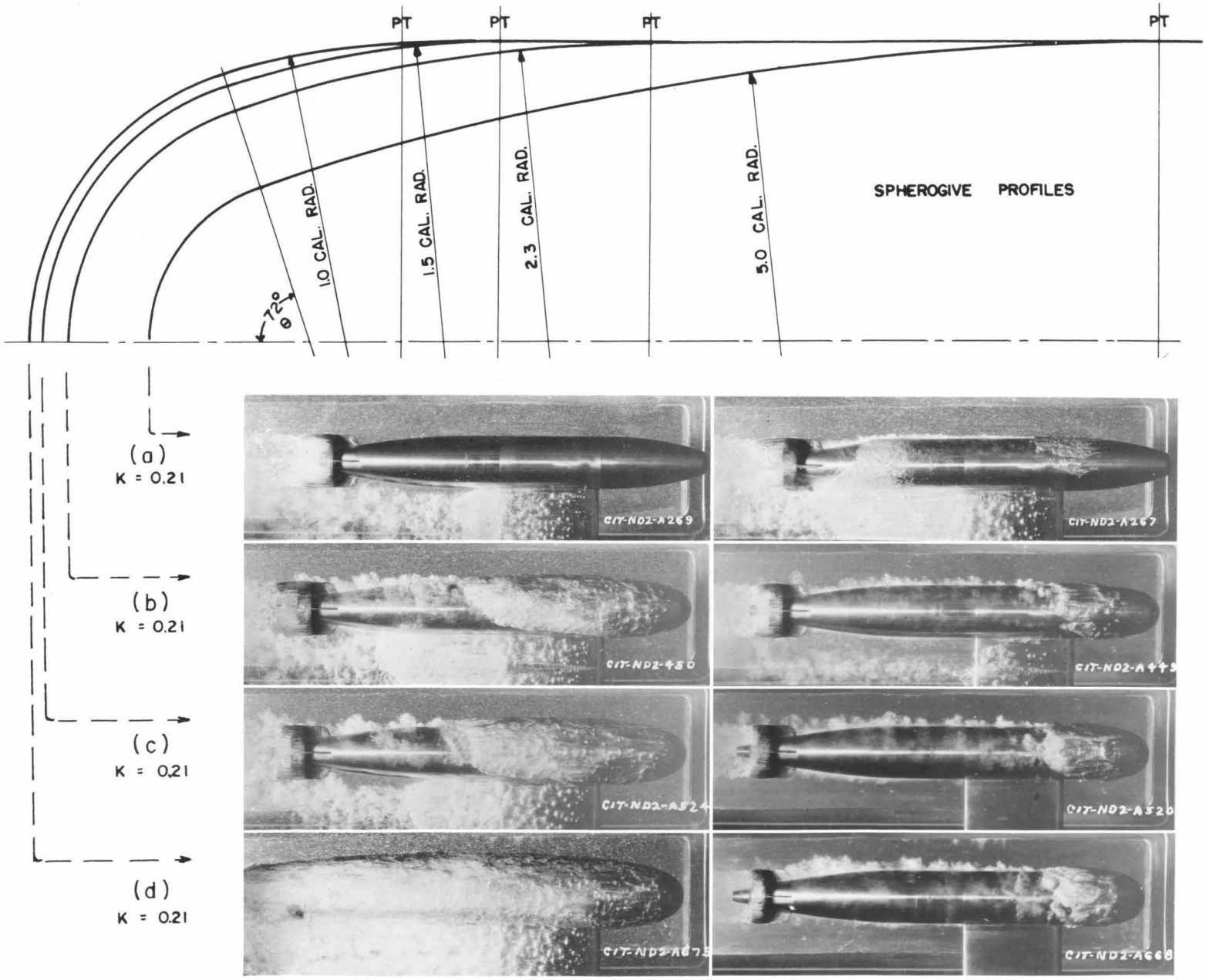

CAVITATION BUBBLES - 72° SPHEROGIVES

FIGURE 25

θ = ½ CENTRAL ANGLE OF SPHERE

(a)  θ = 70° K = 0.17

(b) 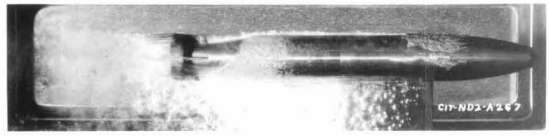 θ = 72° K = 0.17

(c)  θ = 73° K = 0.17

(d)  θ = 74° K = 0.18

(e) 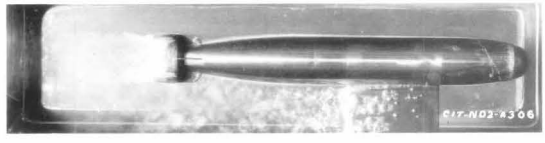 θ = 76° K = 0.25

(f) 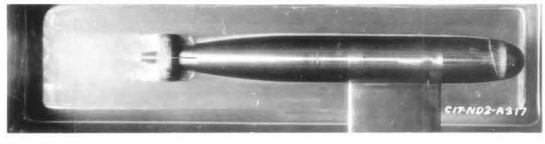 θ = 78° K = 0.32

(g) 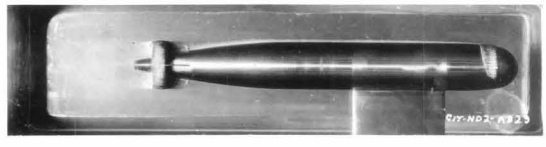 θ = 81° K = 0.41

(h) 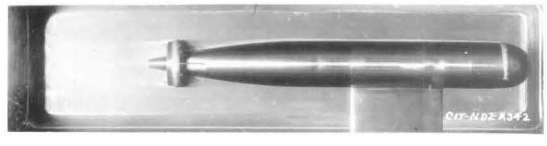 θ = 84° K = 0.55

(i) 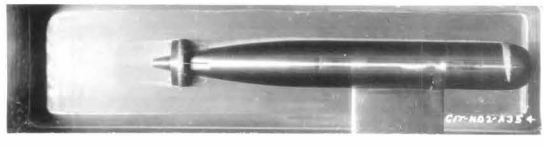 θ = 86° K = 0.57

FAMILY OF 5 CALIBER SPHEROGIVE CAVITATION PHOTOGRAPHS

FIGURE 26

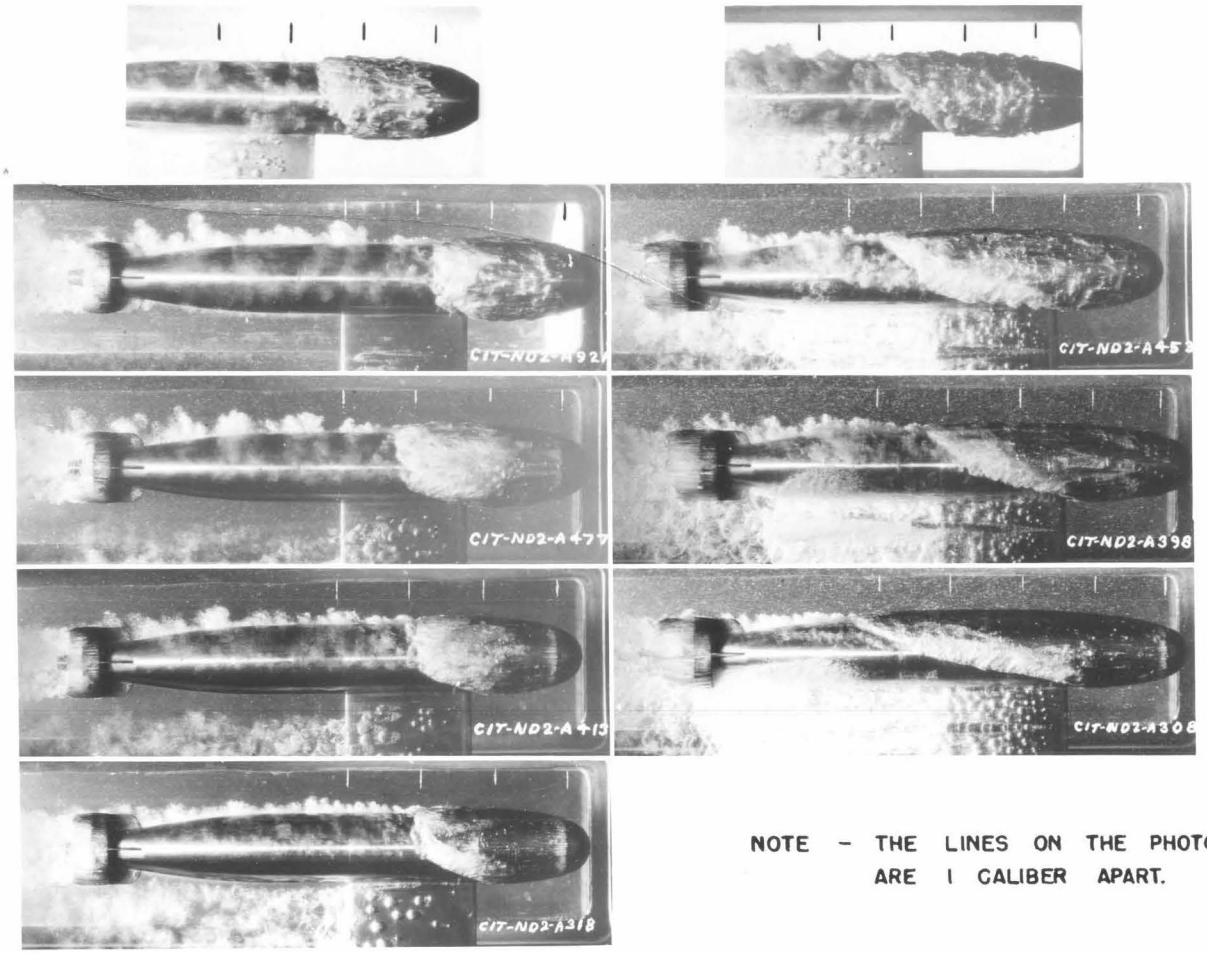

NOTE - THE LINES ON THE PHOTOGRAPHS ARE 1 CALIBER APART.

COMPARISON OF OGIVE AND SPHEROGIVE BUBBLES

FIGURE 27

4. The cavitation bubble originating on a spherical tip develops faster as K is reduced than one starting at the same K_i which originates on a surface of larger radius of curvature such as an ogive.

MEASUREMENTS OF PHOTOGRAPHS

All models have been made 2.00 inches in diameter so this can be used as the unit of length for measurements made on photographs. Owing to the unequal horizontal and vertical distortion caused by the lucite window in the tunnel, the diameter of the model will represent 2" in the vertical direction and 1.83" in the horizontal direction.

CONCLUSIONS

Although based on incomplete data, the following conclusions seem to be justified:

1. The incipient cavitation parameter, K_i, for ogive noses drops rapidly as the ogive radius is increased from 0.5 calibers to 1.0 calibers, the decrease being much less pronounced for radii between 1.0 calibers and 8.0 calibers.

2. The radius of the ogive drawn to the forward edge of a well developed cavitation bubble makes an angle of approximately 86° with the axis of the nose. This angle seems to be constant for all noses investigated.

3. The incipient cavitation parameter, K_i, increases rapidly with an increase in yaw angle. For a hemispherical nose K_i increases from 0.75 for zero yaw to 1.01 for 6° yaw.

4. Photographs of well developed bubbles on a hemispherical nose indicate that the plane of the forward edge of the bubble remains practically at right angles to the direction of travel for yaw angles up to at least 6°.

5. When the sphere segment on spherogive noses is large compared to the ogive, cavitation occurs first on the sphere so that the inception and subsequent growth of the cavitation bubble depend only on the sphere size. When the sphere segment is small compared to the ogive, cavitation occurs first on the ogive and the inception and subsequent bubble growth depend on the ogive and are independent of the sphere size. The critical sphere size dividing the two behaviors is different for different spherogive families. For the 5.0 caliber family of spherogives, this critical sphere size corresponds to a half-sphere angle (θ) of about 72°, and for the 1.0 caliber family, this angle is about 60°.

6. Based on measurements of photographs, it appears that the maximum diameter of the full cavitation bubble on spherogive noses varies directly with the radius of the sphere regardless of the ogive radius.

7. For a given family of spherogives, based on a constant ogive radius, the value of K for incipient cavitation (K_i) will be determined by the half spherical angle. The more blunt the nose, the higher the value of K_i.

APPENDIX

DEFINITIONS

YAW ANGLE, ψ

The angle, in a horizontal plane, which the axis of the projectile makes with the direction of motion. Looking down on the projectile, yaw angles in a clockwise direction are positive (+) and in a counterclockwise direction, negative (-).

PITCH ANGLE, α

The angle, in a vertical plane, which the axis of the projectile makes with the direction of motion. Pitch angles are positive (+) when the nose is up and negative (-) when the nose is down.

LIFT, L

The force, in pounds, exerted on the projectile normal to the direction of motion and in a vertical plane. The lift is positive (+) when acting upward and negative (-) when acting downward.

CROSS FORCE, C

The force, in pounds, exerted on the projectile normal to the direction of motion and in a horizontal plane. The cross force is positive when acting in the same direction as the displacement of the projectile nose for a positive yaw angle, i.e., to an observer facing in the direction of travel, a positive cross force acts to the right.

DRAG, D

The force, in pounds, exerted on the projectile parallel with the direction of motion. The drag is positive when acting in a direction opposite to the direction of motion.

MOMENT, M

The torque, in foot pounds, tending to rotate the projectile about a transverse axis. Yawing moments tending to rotate the projectile in a clockwise direction (when looking down on the projectile) are positive (+), and those tending to cause counterclockwise rotation are negative (-). Pitching moments tending to rotate the projectile in a clockwise direction (when looking at the projectile from the port side) are positive (+), and those tending to cause counterclockwise rotation are negative (-).

In accordance with this sign convention a moment has a destabilizing effect when it has the same sign as the yaw angle or the opposite sign of the pitch angle.

In all model tests the moment is measured about the point of support. Moments about the center of gravity of the projectile have the symbol, M_{cg}.

NORMAL COMPONENT, N

The sum of the components of the drag and cross force acting normal to the axis of the projectile. The value of the normal component is given by the following:

$$N = D \sin \psi + C \cos \psi \qquad (1)$$

in which

N = Normal component in lbs

D = Drag in lbs

C = Cross force in lbs

ψ = Yaw angle in degrees

CENTER OF PRESSURE, CP

The point in the axis of the projectile at which the resultant of all forces acting on the projectile is applied.

CENTER-OF-PRESSURE ECCENTRICITY, e

The distance between the center of pressure (CP) and the center of gravity (CG) expressed as a decimal fraction of the length (l) of the projectile. The center-of-pressure eccentricity is derived as follows:

$$e = (l_{cp} - l_{cg}) \frac{1}{l} = \frac{1}{l} \frac{M_{cg}}{N} \qquad (2)$$

in which

e = Center-of-pressure eccentricity

l = Length of projectile in feet

l_{cg} = Distance from nose of projectile to CG in feet

l_{cp} = Distance from nose of projectile to CP in feet

COEFFICIENTS

The three force and moment coefficients used are derived as follows:

Drag coefficient, $$C_D = \frac{D}{\rho \frac{V^2}{2} A_D} \quad (3)$$

Cross force coefficient, $$C_C = \frac{C}{\rho \frac{V^2}{2} A_D} \quad (4)$$

Moment coefficient, $$C_M = \frac{M}{\rho \frac{V^2}{2} A_D l} \quad (5)$$

in which

D = Measured drag force in lbs

C = Measured cross force in lbs

ρ = Density of the fluid in slugs/cu ft = w/g

w = Specific weight of the fluid in lbs/cu ft

g = Acceleration of gravity in ft/sec^2

A_D= Area in sq ft at the maximum cross section of the projectile taken normal to the geometric axis of the projectile

V = Mean relative velocity between the water and the projectile in ft/sec

M = Moment, in foot-pounds, measured about any particular point on the geometric axis of the projectile

l = Overall length of the projectile in feet

CONTROL ANGLE

In considering the effect of rudders on static stability, either in yaw or pitch, the term "control angle" is used to denote the yaw below which a given rudder setting with opposite sign to the yaw will tend to return the projectile to zero yaw, and above which the yaw will further increase. The control angle is useful for indicating the effectiveness of rudders and for comparing the static stability of different projectiles with equal rudder settings.

RUDDER EFFECT

The total increase or decrease in moment coefficient, at a given yaw or pitch angle, resulting from a given rudder setting. This increase or decrease in moment coefficient is measured from the moment coefficient curve for neutral rudder setting.

REYNOLDS NUMBER

In comparing hydraulic systems involving only friction and inertia forces, a factor called Reynolds number is of great utility. This is defined as follows:

$$R = \frac{lV}{\nu} = \frac{lV\rho}{\mu} \qquad (6)$$

in which

R = Reynolds number

l = Overall length of projectile, feet

V = Velocity of projectile, feet per sec

ν = Kinematic viscosity of the fluid, sq ft per sec = μ/ρ

ρ = Mass density of the fluid in slugs per cu ft

μ = Absolute viscosity in pound-seconds per sq ft

Two geometrically similar systems are also dynamically similar when they have the same value of Reynolds number. For the same fluid in both cases, a model with small linear dimensions must be used with correspondingly large velocities. It is also possible to compare two cases with widely differing fluids provided l and V are properly chosen to give the same value of R.

CAVITATION PARAMETER

In the analysis of cavitation phenomena, the cavitation parameter has been found very useful. This is defined as follows:

$$K = \frac{P_L - P_B}{\rho \frac{V^2}{2}} \qquad (7)$$

in which

K = Cavitation parameter

P_L = Absolute pressure in the undisturbed liquid, lbs/sq ft

P_B = Vapor pressure corresponding to the water temperature, lbs/sq ft

V = Velocity of the projectile, ft/sec

COEFFICIENTS

The three force and moment coefficients used are derived as follows:

Drag coefficient, $$C_D = \frac{D}{\rho \frac{V^2}{2} A_D} \quad (3)$$

Cross force coefficient, $$C_C = \frac{C}{\rho \frac{V^2}{2} A_D} \quad (4)$$

Moment coefficient, $$C_M = \frac{M}{\rho \frac{V^2}{2} A_D l} \quad (5)$$

in which

D = Measured drag force in lbs

C = Measured cross force in lbs

ρ = Density of the fluid in slugs/cu ft = w/g

w = Specific weight of the fluid in lbs/cu ft

g = Acceleration of gravity in ft/sec^2

A_D= Area in sq ft at the maximum cross section of the projectile taken normal to the geometric axis of the projectile

V = Mean relative velocity between the water and the projectile in ft/sec

M = Moment, in foot-pounds, measured about any particular point on the geometric axis of the projectile

l = Overall length of the projectile in feet

CONTROL ANGLE

In considering the effect of rudders on static stability, either in yaw or pitch, the term "control angle" is used to denote the yaw below which a given rudder setting with opposite sign to the yaw will tend to return the projectile to zero yaw, and above which the yaw will further increase. The control angle is useful for indicating the effectiveness of rudders and for comparing the static stability of different projectiles with equal rudder settings.

RUDDER EFFECT

The total increase or decrease in moment coefficient, at a given yaw or pitch angle, resulting from a given rudder setting. This increase or decrease in moment coefficient is measured from the moment coefficient curve for neutral rudder setting.

REYNOLDS NUMBER

In comparing hydraulic systems involving only friction and inertia forces, a factor called Reynolds number is of great utility. This is defined as follows:

$$R = \frac{lV}{\nu} = \frac{lV\rho}{\mu} \qquad (6)$$

in which

R = Reynolds number

l = Overall length of projectile, feet

V = Velocity of projectile, feet per sec

ν = Kinematic viscosity of the fluid, sq ft per sec = μ/ρ

ρ = Mass density of the fluid in slugs per cu ft

μ = Absolute viscosity in pound-seconds per sq ft

Two geometrically similar systems are also dynamically similar when they have the same value of Reynolds number. For the same fluid in both cases, a model with small linear dimensions must be used with correspondingly large velocities. It is also possible to compare two cases with widely differing fluids provided l and V are properly chosen to give the same value of R.

CAVITATION PARAMETER

In the analysis of cavitation phenomena, the cavitation parameter has been found very useful. This is defined as follows:

$$K = \frac{P_L - P_B}{\rho \frac{V^2}{2}} \qquad (7)$$

in which

K = Cavitation parameter

P_L = Absolute pressure in the undisturbed liquid, lbs/sq ft

P_B = Vapor pressure corresponding to the water temperature, lbs/sq ft

V = Velocity of the projectile, ft/sec

ρ = mass density of the fluid in slugs per cu ft = w/g

w = weight of the fluid in lbs per cu ft

g = acceleration of gravity

Note that any homogeneous set of units can be used in the computation of this parameter. Thus, it is often convenient to express this parameter in terms of the head, i.e.,

$$K = \frac{h_L - h_B}{\frac{V^2}{2g}} \qquad (8)$$

where

h_L = Submergence plus the barometric head, ft of water

h_B = Pressure in the bubble, ft of water

It will be seen that the numerator of both expressions is simply the net pressure acting to collapse the cavity or bubble. The denominator is the velocity pressure. Since the entire variation in pressure around the moving body is a result of the velocity, it may be considered that the velocity head is a measure of the pressure available to open up a cavitation void. From this point of view, the cavitation parameter is simply the ratio of the pressure available to collapse the bubble to the pressure available to open it. If the K for incipient cavitation is considered, it can be interpreted to mean the maximum reduction in pressure on the surface of the body measured in terms of the velocity head. Thus, if a body starts to cavitate at the cavitation parameter of one, it means that the lowest pressure at any point on the body is one velocity head below that of the undisturbed fluid.

The shape and size of the cavitation bubbles for a specific projectile are functions of the cavitation parameter. If p_B is taken to represent the gas pressure within the bubble instead of the vapor pressure of the water, as in normal investigations, the value of K obtained by the above formula will be applicable to an air bubble. In other words, the behavior of the bubble will be the same whether the bubble is due to cavitation, the injection of exhaust gas, or the entrainment of air at the time of launching.

The following chart gives values of the cavitation parameter as a function of velocity and submergence in sea water.

GENERAL DISCUSSION OF STATIC STABILITY

Water tunnel tests are made under steady flow conditions, consequently the results only indicate the tendency of the steady state hydrodynamic couples and forces to cause the projectile to return to or move away from its equilibrium position after a

disturbance. Dynamic couples and forces including either positive or negative damping are not obtained. If the hydrodynamic moments are restoring the projectile, then it is said to be statically stable, if nonrestoring, statically unstable. In the discussion of static stability the actual motion following a perturbation is not considered at all. In fact, the projectile may oscillate continuously about an equilibrium position without remaining in it. In this case it would be statically stable, but would have zero damping and hence, be dynamically unstable. With negative damping a projectile would oscillate with continually increasing applitude following an initial perturbation even though it were statically stable. Equilibrium is obtained if the sum of the hydrodynamic, buoyant, and propulsive moments equal zero. In general, propulsive thrusts act through the center of gravity of the projectile so only the first two items are important.

If a projectile is rotating from its equilibrium position so as to increase its yaw angle positively, the moment coefficient must increase negatively (according to the sign convention adopted) in order that it be statically stable. Therefore, for projectiles without controls or with fixed control surfaces, a negative slope of the curve of moment coefficient vs yaw gives static stability and a positive slope gives instability. For a projectile without controls, static stability is necessary for a successful flight unless stability is obtained by spinning as in the case of rifle shells. For a projectile with controls, stabilizing moments can be obtained by adjusting the control surfaces, and the slope of the moment coefficient, as obtained with fixed rudder position, need not give static stability. Where buoyancy either acts at the center of gravity or can be neglected, equilibrium is obtained when the hydrodynamic moment coefficient equals zero. For symmetrical projectiles this occurs at zero yaw angle, i.e., when the projectile axis is parallel to the trajectory. For nonsymmetrical projectiles, such as a torpedo when the rudders are not neutral, the moment is not zero at zero yaw but vanishes at some definite angle of attack. Where buoyancy cannot be neglected equilibrium is obtained when $C_M = -C_{Buoyancy}$, and the axis of the projectile is at some angle with the trajectory.

For symmetrical projectiles the degree of stability or instability can be obtained from the center-of-pressure curves. If the center of pressure falls behind the center of gravity, a restoring moment exists giving static stability. If the center of pressure falls ahead of the center of gravity, the moment is nonrestoring, and the projectile will be statically unstable. The degree of stability or instability is indicated approximately by the distance between the center of gravity and the center of pressure. In general, for nonsymmetrical projectiles, the cross force or lift is not zero when the moment vanishes so that the center of pressure curve is not symmetrical and the simple rules just stated cannot be used to determine whether or not the projectile will be stable. In such cases careful interpretation of the moment curves is a more satisfactory method of determining stability relationship.

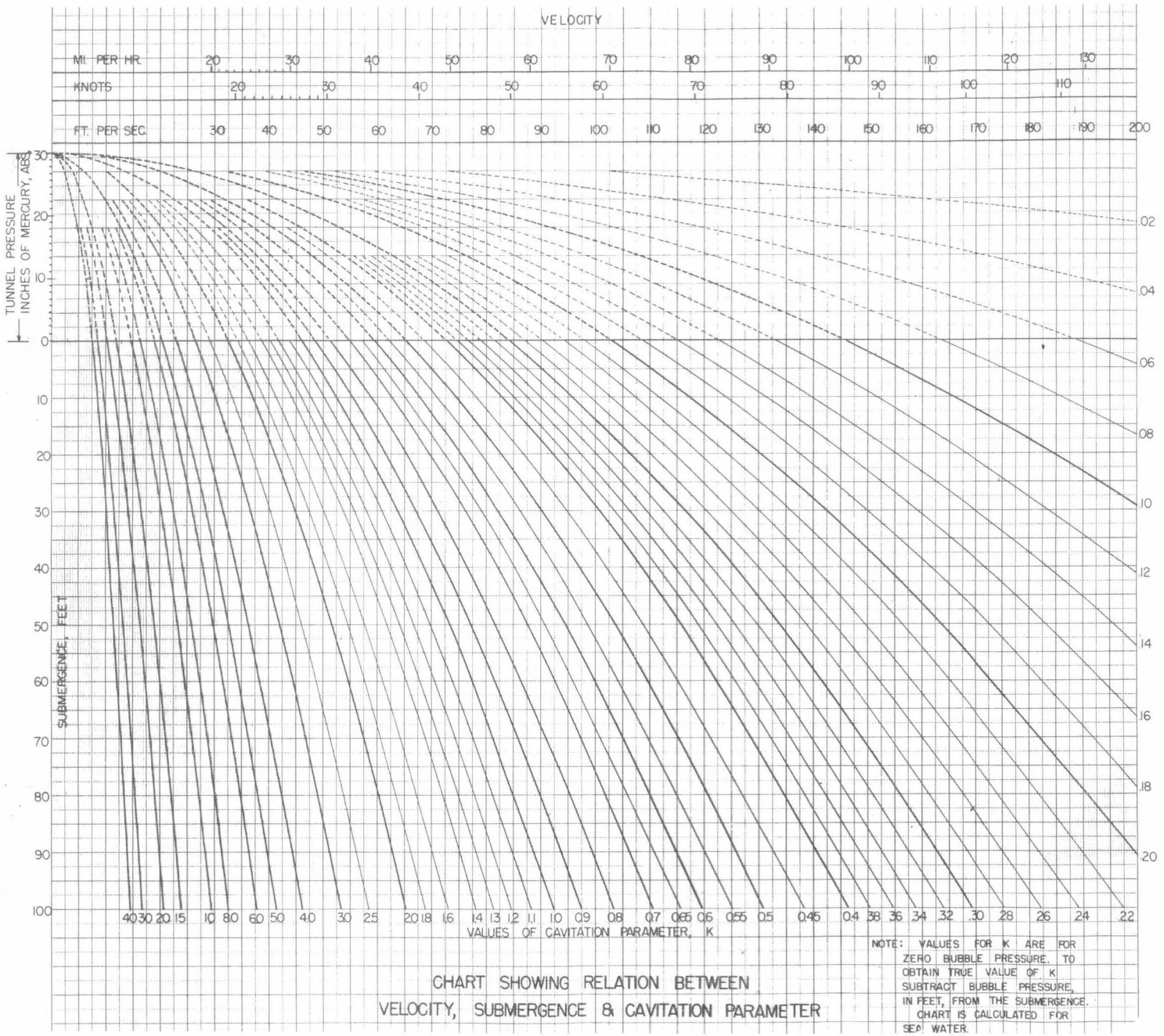

CHART SHOWING RELATION BETWEEN
VELOCITY, SUBMERGENCE & CAVITATION PARAMETER

CONFIDENTIAL